isvr Institute of Sound and Vibration Research

Power Transmission between Long-wavelength Sources and Short-wavelength Receivers

L. Ji, B.R. Mace and R.J. Pinnington

ISVR Technical Memorandum 876

December 2001

University of Southampton

SCIENTIFIC PUBLICATIONS BY THE ISVR

Technical Reports are published to promote timely dissemination of research results by ISVR personnel. This medium permits more detailed presentation than is usually acceptable for scientific journals. Responsibility for both the content and any opinions expressed rests entirely with the author(s).

Technical Memoranda are produced to enable the early or preliminary release of information by ISVR personnel where such release is deemed to the appropriate. Information contained in these memoranda may be incomplete, or form part of a continuing programme; this should be borne in mind when using or quoting from these documents.

Contract Reports are produced to record the results of scientific work carried out for sponsors, under contract. The ISVR treats these reports as confidential to sponsors and does not make them available for general circulation. Individual sponsors may, however, authorize subsequent release of the material.

UNIVERSITY OF SOUTHAMPTON

INSTITUTE OF SOUND AND VIBRATION RESEARCH

DYNAMICS GROUP

Power Transmission between Long-wavelength Sources and Short-wavelength Receivers

by

L. Ji, B.R. Mace and R.J. Pinnington

ISVR Technical Memorandum No: 876

December 2001

Contents

Abstract

This study is an attempt to approximate simply and accurately the power transmission of complex built-up structures consisting of both long- and short-wavelength substructures. For practical concern, the long-wavelength substructures are usually to be the sources, while the short wavelength substructures to be the receivers. For discrete coupling cases the multi-pole method and a new technique – the power mode method, have been investigated. Three approximation expressions for the transmitted power have been derived base on this power mode theory. For line-coupled cases, a foundation consisting of a beam-stiffened plate with the excitation applied to the beam is studied. The power transmission from the source beam to the plate receiver are investigated for three cases: Case 1, an infinite beam attached to an infinite plate, is investigated by the Fourier Transform and wave-based methods; Case 2, a finite beam attached to an infinite plate, is investigated by a combined modal analysis/Fourier Transform approach as well as the locally reacting impedance method; and Case 3, a finite beam attached to a finite plate, is investigated by the modal analysis theory. Simple expressions for the power transmission as well as the modified dynamic response of the source beam have been derived. Furthermore the effects of coupling the plate to the beam are discussed and compared with the results obtained from the "Fuzzy" theory.

1. Introduction

An understanding of the vibration power transmission in complex built-up systems, composed of both source and receiver substructures, is essential in the attempt to solve the many vibration problems of practical concern, such as vehicles, aircraft structures, mechanical equipment, etc. In the study of power transmission from source substructures to receiver substructures, two general cases are involved [1]: ideal force/velocity sources and general linear sources.

A force source is one that generates forces regardless of the velocity responses of the receiver, and a velocity source generates velocities which can not be affected by the force responses of the receiver. Force-source-like behaviour may, for example, be observed at mounting points at which rigid frames of unbalanced rotating machines are attached to other structures. Velocity-source-like behaviour may be produced, for example, by the action of a piston in a reciprocating machine operating at constant rotational speed. Most realistic sources depart from these ideal behaviours, of course. It is usual to consider a general linear source, whose force output and velocity output are linearly related by

$$F_S = F_0 - \frac{V_S}{M_S} = \frac{V_0 - V_S}{M_S} \tag{1.1}$$

where F_0 and V_0 are the outputs of a force source and of a velocity source, and F_S and V_S are the force and velocity outputs of the general source, and M_S denotes its mobility. In [1], such a general linear source is illustrated by the two equivalent representations shown in Figure 1.1.

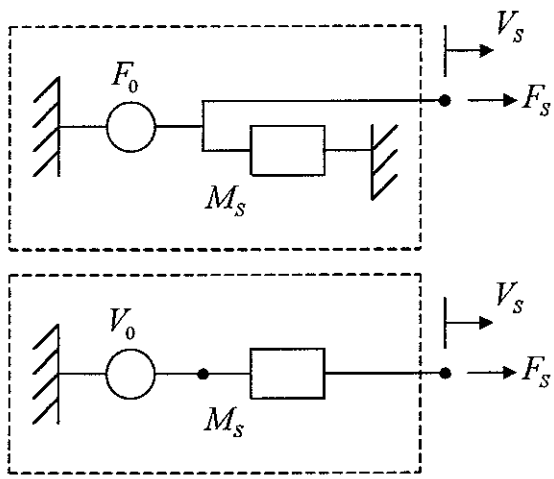

Figure 1.1 Two equivalent representations of a general linear force

It can be seen then a force source corresponds to $M_S = \infty$, and a velocity source to $M_S = 0$, i.e., ideal force/velocity sources are only special cases of general linear sources.

When a general line force source is attached to a receiver with an input mobility M_R as shown in Figure 1.2, the interface force response F_I and the velocity response V_I is then related by

$$V_I = F_I M_R = \frac{F_0}{M_S^{-1} + M_R^{-1}} = \frac{V_0}{1 + M_S / M_R} \tag{1.2}$$

It can be seen from the above equation that the outputs of source depend on both the properties of the source and the receiver. Equation (1.2) also denotes that $F_I = F_0$ for a force source, and $V_I = V_0$ for a velocity source.

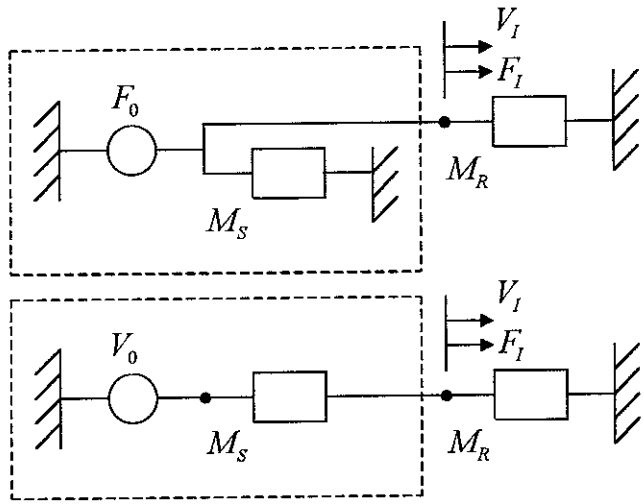

Figure 1.2 Two equivalent representations of a general linear force attached to a receiver

Some investigations of vibration power transmission induced by ideal force/velocity source excitations have been reported in [16]. This study is therefore proposed to investigate the vibration power transmission from general linear sources to receivers, which are more complex than the ideal force/velocity source excitation cases. Since in geometries of practical interest, the case of stiff source/flexible receiver prevails, a typical complex built-up system can be considered as composed of a long-wavelength and/or low-modal-density source substructure and a short-wavelength and/or high-modal-density receiver substructure.

To model the dynamic characteristic of such structures at higher frequencies, neither deterministic methods [2-3] (e.g. FEA) nor stochastic approaches [4-5] (e.g. SEA) are

able to predict the vibration behaviour with acceptable accuracy. In the low frequency range deterministic methods can be used to predict the vibration behaviour of coupled structures very accurately with same computational cost. However, at higher frequency, in what might be termed the 'mid-frequency' range, the wavelength of the system deformation reduces as frequency increases and the size of the model increases accordingly. In the context of FEA, it is generally considered that approximately four to eight elements (depend on the related vibration shape functions) must be used to adequately resolve each structural wavelength, and this can and does lead to unfeasibly large models at high frequencies. The Statistical Energy Analysis (SEA) method has been successfully applied to the high-frequency vibration analysis of coupled systems, provided that each subsystem ideally contains a number of resonant modes over the analysis frequency band of interest, i.e., the wavelength of the subsystem deformation is of the same order as, or less than, the dimensions of the subsystem. The primary aim of the analysis is to estimate the distribution of vibration energy among the coupled subsystems. In the mid-frequency range, i.e. the frequencies are not high enough to make the wavelengths of all subsystems to be sufficiently short, this high-frequency, energy-based approach will become too broad-brush and lose all details of the system vibration behaviour.

Some modal reduction techniques [6-7] have been developed to deal with the coupled responses of such complex built-up structures. As the most commonly used one, the FRF-based sub-structuring method has been shown very useful if the frequency response functions of all the subsystems of a built-up structure can be obtained easily (either analytically or experimentally). The fundamental concept of this technique is to utilize the individual uncoupled component FRFs to construct the total system response based on dynamic compliance formulation. The procedure is reviewed below for a general source/receiver system.

For the source substructure, its velocity responses at the interface degrees of freedom, by referring to Figure 2.1 and equation (1.2), can be written as

$$\mathbf{V}_I = \mathbf{V}_{sf} - \mathbf{M}_S \mathbf{F}_I \tag{1.3}$$

where $\mathbf{F}_I$ is a vector of interface force applied to the source by the receiver, $\mathbf{M}_S$ the uncoupled mobility matrix of the source at the interface degrees of freedom (DOFs), and $\mathbf{V}_{sf}$ the free velocity vector of the source at the interface DOFs before it is coupled with the receiver so that

$$\mathbf{V}_{sf} = \mathbf{M}_{0S}\mathbf{F}_0 \tag{1.4}$$

where $\mathbf{F}_0$ is a vector comprising the force excitations applied to the source structure, and $\mathbf{M}_{0S}$ the source mobility matrix from the excitation coordinates to the coupling coordinates. The compatibility and equilibrium boundary conditions at the interface also give

$$\mathbf{V}_I = \mathbf{M}_R\mathbf{F}_I \tag{1.5}$$

where $\mathbf{M}_R$ is the uncoupled mobility matrix of the receiver at the interface. The dynamic response of the receiver at the interface DOFs can then be defined as

$$\mathbf{F}_I = \left(\mathbf{M}_S + \mathbf{M}_R\right)^{-1}\mathbf{V}_{sf} \tag{1.6}$$

$$\mathbf{V}_I = \mathbf{M}_R\left(\mathbf{M}_S + \mathbf{M}_R\right)^{-1}\mathbf{V}_{sf} \tag{1.7}$$

The power transmitted from the source to the receiver thus can be expressed as

$$P = \frac{1}{2}\mathrm{Re}\left\{\mathbf{F}_I{}^H\mathbf{V}_I\right\} = \frac{1}{2}\mathrm{Re}\left\{\mathbf{V}_{sf}{}^H\left[\left(\mathbf{M}_S + \mathbf{M}_R\right)^{-1}\right]^H\mathbf{M}_R\left(\mathbf{M}_S + \mathbf{M}_R\right)^{-1}\mathbf{V}_{sf}\right\} \tag{1.8}$$

where H denotes complex conjugate of the matrix. Equation (1.8) can be written as

$$P = \frac{1}{2}\mathbf{V}_{sf}{}^H\,\mathrm{Re}\left\{\mathbf{Z}_{coup}\right\}\mathbf{V}_{sf} \tag{1.9}$$

where,

$$\mathbf{Z}_{coup} = \left[\left(\mathbf{M}_S + \mathbf{M}_R\right)^{-1}\right]^H\mathbf{M}_R\left(\mathbf{M}_S + \mathbf{M}_R\right)^{-1} \tag{1.10}$$

A full description of the power transmission from a source to a receiver by this approach inherently requires evaluation of many terms as well as a matrix inversion. This can be computationally prohibitive, especially when the number of the interface degrees of freedom is very large (e.g. line coupling, which can be regarded as being discrete point connection, if the points are close enough). Also, inaccurate results may be obtained during the matrix inversion if the mobility matrix is ill-conditioned. Therefore this technique could be rather problematic for many interface DOFs coupling cases.

It is generally more useful to approximate the main properties of the power transmission rather than to predict precisely its detailed response, since the theoretical results can only rarely be applied to practical structure-borne sound problems [8]. As frequency increases the system response becomes increasingly sensitive to geometrical imperfections, so that even a very detailed deterministic mathematical model based on the nominal system properties may not yield a reliable response

prediction. Although some specialist methods [9-15] have been developed by different authors to approximate the transmitted power from stiff sources to flexible receivers, certain significant limitations exist in their applications, especially for the line-coupling cases. It is true to say more research is required before a complete and generally accepted approximate theory is developed. Therefore the emphasis in this study is to approximate simply and accurately the power transmission between stiff sources and flexible receivers coupled by either discrete or line couplings. Since many of the basic features of structures of practical concern can be reduced to relatively simple configurations of beams and plates, for line-coupling cases a typical foundation consisting of beam-stiffened plate with the excitation applied to the beam is therefore investigated in the first instance. Extending the methods to more complex geometries is the subject of the further research.

For discrete point-coupling cases, both the multi-pole and the power mode methods have been used to simplify the power transmission prediction from a stiff source to a flexible receiver. For line-couplings e.g. beam-stiffened plate systems, three cases are investigated: Case 1, an infinite beam attached to an infinite plate, is investigated by Fourier Transform method and wave analysis method; Case 2, a finite beam attached to an infinite plate, is investigated by a combined modal analysis and Fourier Transform method; and Case 3, a finite beam attached to a finite plate, is investigated by modal analysis method. Simplified expressions for the power transmission are derived, and their accuracy verified by comparing with numerical results by the FRF-based sub-structuring approach. Moreover the coupling effects of the plate to the beam are analysed quantitatively and compared with those obtained by fuzzy structure theory [13-14].

It is expected that these approximate techniques can be further generalized so as to form a complete approximation approach applicable to any system composed of both long-wavelength (low modal density) and short-wavelength (high modal density) substructures. This forms the next stage of this study.

2. Power transmission through discrete couplings, Part I: Application of the multipole method

2.1 The multipole theory

The multipole method, which is first developed in [9], is to attempt to simplify the modelling and measurement of power transmitted into machine mounting configurations, by describing the source vibrations as moving in a set of vibration poles and the receiver as a set of polar mobilities or impedances. The main theory of this method is reviewed below.

Let $\mathbf{\Phi}$ be an $N \times N$ Hadamard matrix, i.e., a matrix of orthogonal functions and whose elements are ± 1. The matrix $\mathbf{\Phi}$ implies such relations

$$\mathbf{\Phi} = \mathbf{\Phi}^T, \ \mathbf{\Phi}^{-1} = \frac{1}{N}\mathbf{\Phi} \tag{2.1}$$

Then let the set of force excitations $\mathbf{F}$ be weighted by $\mathbf{\Phi}$ to give a new set of polar forces $\mathbf{Q}$ defined by

$$\mathbf{Q} = \mathbf{\Phi F} \tag{2.2}$$

Accordingly the polar mobility matrix can be defined by

$$\mathbf{M}_n = \frac{1}{N^2}\mathbf{\Phi M \Phi} \tag{2.3}$$

Then the power transmitted by multipoint forces $\mathbf{F}$ is given as

$$P = \frac{1}{2}\mathrm{Re}\left\{\mathbf{F}^H \mathbf{M F}\right\} = \frac{1}{2}\mathrm{Re}\left\{\mathbf{Q}^H \mathbf{M}_n \mathbf{Q}\right\} \tag{2.4}$$

Likewise, a set of polar velocities $\mathbf{U}$ as well as the polar impedance matrix can be expressed as

$$\mathbf{U} = \frac{1}{N}\mathbf{\Phi V} \tag{2.5}$$

$$\mathbf{Z}_n = \mathbf{M}_n^{-1} \tag{2.6}$$

The power transmitted by the set of velocity excitations is then given as

$$P = \frac{1}{2}\mathrm{Re}\left\{\mathbf{V}^H \mathbf{M}^{-1} \mathbf{V}\right\} = \frac{1}{2}\mathrm{Re}\left\{\mathbf{U}^H \mathbf{Z}_n \mathbf{U}\right\} \tag{2.7}$$

If both the receiver structure and the excitation points are symmetric, $\mathbf{M}_n$ will be diagonal and equal to $\mathbf{\Lambda}$, i.e.,

$$\mathbf{\Lambda} = \frac{1}{N^2}\mathbf{\Phi}\mathbf{M}\mathbf{\Phi} \tag{2.8}$$

The power transmission to the receiver then can be written as

$$P = \frac{1}{2}\mathbf{Q}^H \mathrm{Re}\{\mathbf{\Lambda}\}\mathbf{Q} = \frac{1}{2}\mathbf{U}^H \mathrm{Re}\{\mathbf{\Lambda}^{-1}\}\mathbf{U} \tag{2.9}$$

Equation (2.9) shows that the vibration power transmitted by N forces/velocities can be regarded as the power transmitted by N independent poles of vibration, where the n th polar power is given by

$$P_n = \frac{1}{2}|Q_n|^2 \mathrm{Re}\{\Lambda_{nn}\} = \frac{1}{2}|U_n|^2 \mathrm{Re}\{\Lambda_{nn}^{-1}\} \tag{2.10}$$

2.2 Power transmission approximation using the multipole method

2.2.1 Fully symmetric source/receiver coupled system

For a coupled source/receiver system, if the receiver is fully symmetric, the interface force acting on the receiver, from equation (1.6) and (2.2), can be expressed as the polar force

$$\mathbf{Q} = \left(\mathbf{\Lambda}_{\mathrm{R}} + \frac{1}{N^2}\mathbf{\Phi}\mathbf{M}_{\mathrm{S}}\mathbf{\Phi}\right)^{-1}\mathbf{U}_{\mathrm{sf}} \tag{2.11}$$

where $\mathbf{\Lambda}_{\mathrm{R}}$ is the polar mobility matrix of the receiver, and $\mathbf{U}_{\mathrm{sf}}$ is a set of free polar velocities, determined by equations (2.3) and (2.5), respectively, i.e.,

$$\mathbf{\Lambda}_{\mathrm{R}} = \frac{1}{N^2}\mathbf{\Phi}\mathbf{M}_{\mathrm{R}}\mathbf{\Phi} \tag{2.12}$$

$$\mathbf{U}_{\mathrm{sf}} = \frac{1}{N}\mathbf{\Phi}\mathbf{V}_{\mathrm{sf}} \tag{2.13}$$

The power transmission to the receiving structure can then be written as

$$P = \frac{1}{2}\mathbf{Q}^H \mathrm{Re}\{\mathbf{\Lambda}_{\mathrm{R}}\}\mathbf{Q} = \sum_{n=1}^{N} P_n \tag{2.14}$$

where P_n is the n th polar power given by

$$P_n = \frac{1}{2}|Q_n|^2 \mathrm{Re}\{\Lambda_{R,nn}\} \tag{2.15}$$

If the source structure is also fully symmetric, we can similarly write

$$\mathbf{\Lambda_S} = \frac{1}{N^2}\mathbf{\Phi M_S \Phi} \tag{2.16}$$

Then $\mathbf{Z_{coup}}$ in expression (1.10) can be written as

$$\mathbf{Z_{coup}} = \frac{1}{N^2}\mathbf{\Phi}\left[\left(\mathbf{\Lambda_S} + \mathbf{\Lambda_R}\right)^H\right]^{-1}\mathbf{\Lambda_R}\left(\mathbf{\Lambda_S} + \mathbf{\Lambda_R}\right)^{-1}\mathbf{\Phi} \tag{2.17}$$

The power transmission is then

$$P = \sum_{n=1}^{N} P_n = \sum_{n=1}^{N} \frac{1}{2}\left|U_{sf,n}\right|^2 \frac{\mathrm{Re}\left\{\Lambda_{R,nn}\right\}}{\left|\Lambda_{R,nn} + \Lambda_{S,nn}\right|^2} \tag{2.18}$$

Thus the power can also be regarded as transmitted by N independent poles of vibration. It can be seen in this case, the multi-pole method has great advantages for simplifying the power transmission estimation from the source to the receiver.

Equation (2.18) also demonstrates that the power transmitted to each pole of the receiver has a direct relation with its corresponding source pole but is independent of other source poles. In this case (both the source and the receiver are fully symmetric), it might be appropriate to characterise the source by a set of free polar velocities, while the receiver is described by a set of 'modified' polar impedances, since the coupling effects between the source and the receiver have to be taken into account.

If either the source, the receiver, or the excitations are not fully symmetric, then generally the transformed polar mobility matrices $\mathbf{\Lambda_S}$ and $\mathbf{\Lambda_R}$ are not diagonal, and hence the transmitted power in equation (2.18) contains also coupled terms, which indicate the couplings between different poles. In these circumstances, the multipole technique seems have no advantage over the FRF-based sub-structuring method. However, in certain cases, the off-diagonal coupling terms may be so small that the polar mobility matrices can almost be regarded as diagonal. Therefore it is possible to yield a valuable approximation using this polar analysis approach.

2.2.2 Asymmetric source/receiver coupled system

For a flexible receiver with high modal overlap so that there is no distinct resonant behaviour, due to high modal density and/or heavy damping, the cross terms of $\mathbf{\Lambda_R}$ in equation (2.12) can be ignored [9], i.e., the polar mobility matrix can be regarded as

diagonal. As far as such flexible receiver structures are concerned, the transmitted power can be simply approximated using equation (2.18) with acceptable accuracy, provided the source structures are fully symmetric.

If the source structure is neither fully symmetric nor has high modal overlap, the cross terms of source polar mobility matrix are usually not small enough to be ignored compared to the diagonal terms. However, if the source structure has much lower mobility compared to that of the receiver, such a relation always holds as

$$\Lambda_{R,nn} >> \Lambda_{S,nn} \tag{2.19}$$

In this case equation (2.18) can be also applicable to approximate the transmitted power.

For other cases, however, the multipole method has no advantages over the FRF-based sub-structuring method.

2.3 Numerical studies

To get more understanding of this polar analysis method as well as to investigate the accuracy of the power transmission approximations made by this approach, some numerical results are presented for a system consisting of a stiff beam connected to a flexible rectangular plate by two discrete points, as shown in Figure 2.1

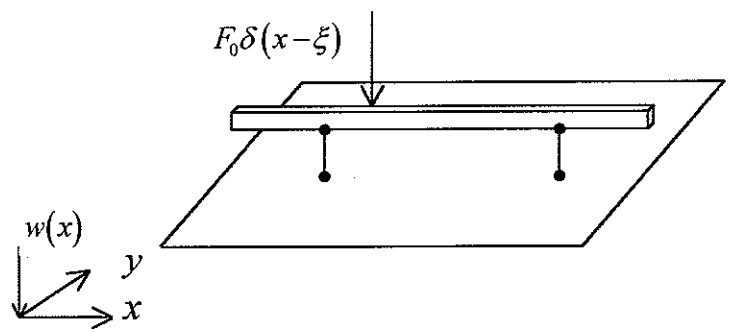

Figure 2.1 Point coupled beam-plate system

For simplicity, both the ends of the beam and the four edges of the rectangular plate are chosen to be simply supported. The material of the system is chosen to be perspex and the relevant properties are listed in Table 2.1. An external point force F_0 acts on the beam at a distance $\xi = 0.73m$ to one end of the beam. Three different coupling cases are investigated: (1) the coupling points are symmetric to both the beam and the plate; (2) the

coupling points are symmetric to the beam but asymmetric to the plate; (3) the coupling points are asymmetric to both the beam and the plate. The locations of the coupling points on the beam and on the plate for the three different cases are listed in Table 2.2. First the mobility method is used so to get the accurate results of power transmission from the beam to the plate, and then the polar analysis approach is used. Comparisons are made in Figure 2.2-2.4 for case 1, Figure 2.5-2.6 for case 2, and Figure 2.7-2.8 for case 3.

Table 2.1 Properties of the numerical beam and plate structures

Structure	Beam	Plate
Dimension sizes	Length=2m; width=0.059m; Height=0.068m	Length=2m; Width=0.9m; Thickness=0.010m
Material properties	Young's modulus=4.4e9 N/m^2; Density=1152kg/m^3; Loss factor=0.05; Poisson's ratio=0.38	

Table 2.2 Locations of the coupling points

	Coupling positions on the beam (m)	Coupling positions on the plate (m)
Case 1	$x_{b1}=0.56$; $x_{b2}=1.44$	$(x_{p1},y_{p1})=(0.56,0.45)$; $(x_{p2},y_{p2})=(1.44,0.45)$
Case 2	$x_{b1}=0.56$; $x_{b2}=1.44$	$(x_{p1},y_{p1})=(0.43,0.45)$; $(x_{p2},y_{p2})=(1.31,0.45)$
Case 3	$x_{b1}=0.43$; $x_{b2}=1.31$	$(x_{p1},y_{p1})=(0.43,0.45)$; $(x_{p2},y_{p2})=(1.31,0.45)$

Figures 2.2–2.3 compared the point- and polar mobilities of the source beam and the receiver plate, respectively. It can be seen that when a structure exhibits resonant behaviour, only one pole dominates at each resonant frequency. Around the first natural frequency of the structure, the monopole dominates. However, when the structure has no distinct resonant behaviour due to, for example, high modal overlap (e.g. Figure 2.3), the values of different poles tend to be close. This is because the point mobility and the

transfer mobility can be very close to each other due to a resonant mode or a long wavelength, thus by the relation of equation (2.3) one of the poles will be much larger than the others. For the high modal overlap areas, however, the point mobility becomes larger than the transfer mobility, and each pole will have a significant effect on the vibration properties of the system. Figure 2.4 shows the relation between the total transmitted power and the power transmitted by each pole. It can be seen that there do exist some frequency ranges where the power is specially related to one pole. For these frequency areas, this polar analysis method will be particularly useful.

Figure 2.5 shows comparisons of the diagonal terms and the off-diagonal cross terms of the polar mobility matrix of the receiver for Case 2. It can be seen that for high modal overlap areas (e.g. the modal overlap factor of the receiver is at least bigger than 1 or the frequency range is above 150 Hz), the cross terms tend to be much less than the diagonal terms. Therefore it is quite reasonable to take the polar mobility matrix of such a receive structure as diagonal. Consequently the power can be also regarded as transmitted by independent poles. Figure 2.6 shows the comparison between the exact result of transmitted power and the approximation made when all the off-diagonal terms of the polar mobility matrix of the receiver are ignored. It can be seen that when the modal overlap factor of the receive structure is more than unity or the frequency range is above 150 Hz, the approximate result is quite accurate.

In Case 3, the source structure is asymmetric and has low modal overlap, the cross terms of source polar mobility matrix are comparable with the diagonal terms, as shown in Figure 2.7, however, it can be seen from Figure 2.8 that equation (2.18) still can be used to make a good approximation due to the source structure being stiff enough compared to the flexible receiver.

2.4 Discussion

Based on the multipole theory, the transmitted power from a source structure to a receiver structure can be approximated with acceptable accuracy using a simple expression of equation (2.18) for the following cases: Case 1, both the source and the receiver structures are fully symmetric; Case, 2, the source structure is fully symmetric and the receiver has high modal overlap with non-distinct resonant behaviour; and Case 3, the source structure is much stiffer than the receiver, which has high modal overlap

with non-distinct resonant behaviour. For other situations, the multipole method has no advantages over the FRF based sub-structuring method.

One may also have noticed that the orders of Hadamard matrices are $N = 2^p, p = 1,2,3\ldots$ but the number of excitation points N may not be related by $N = 2^p$, although four or eight points are relatively common in practical engineering. In [9], it is pointed out that the number of points used may not have to correspond to exact number of excitations but to $N = 2^p$, since the polar mobilities are not very sensitive to the exact positions of the coupling points. This is particularly useful if there are a large number of excitation points and some of them are spaced within one half wavelength. But for higher frequencies where all the excitations points are spaced more than half of the wavelengths with each other, no such a simplification can be made.

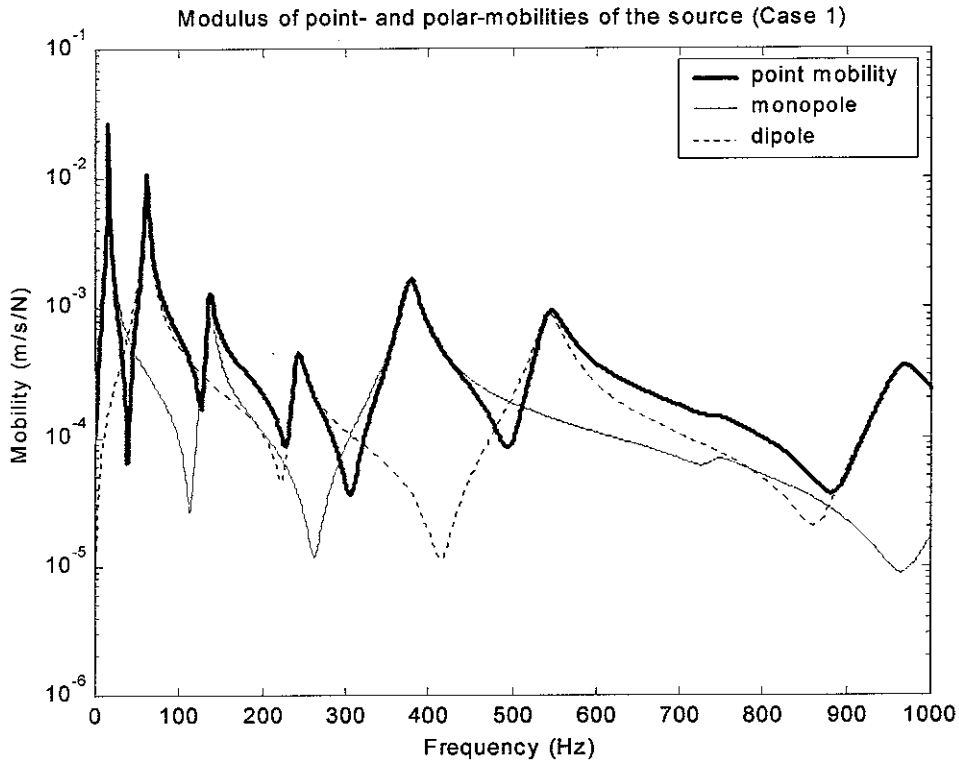

Figure 2.2

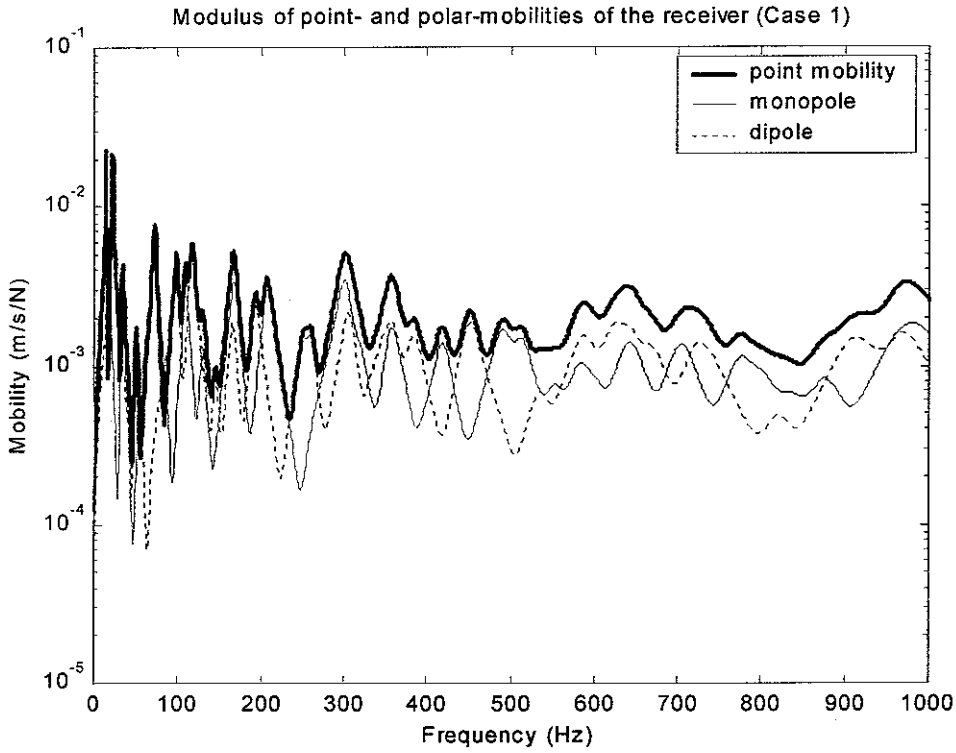

Figure 2.3

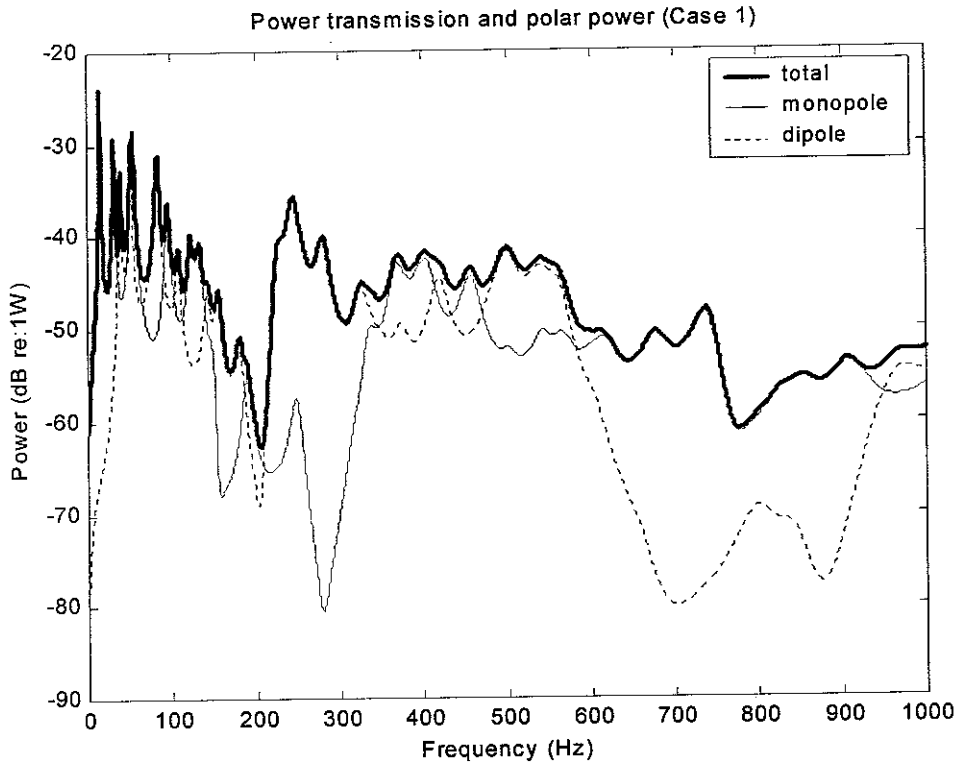

Figure 2.4

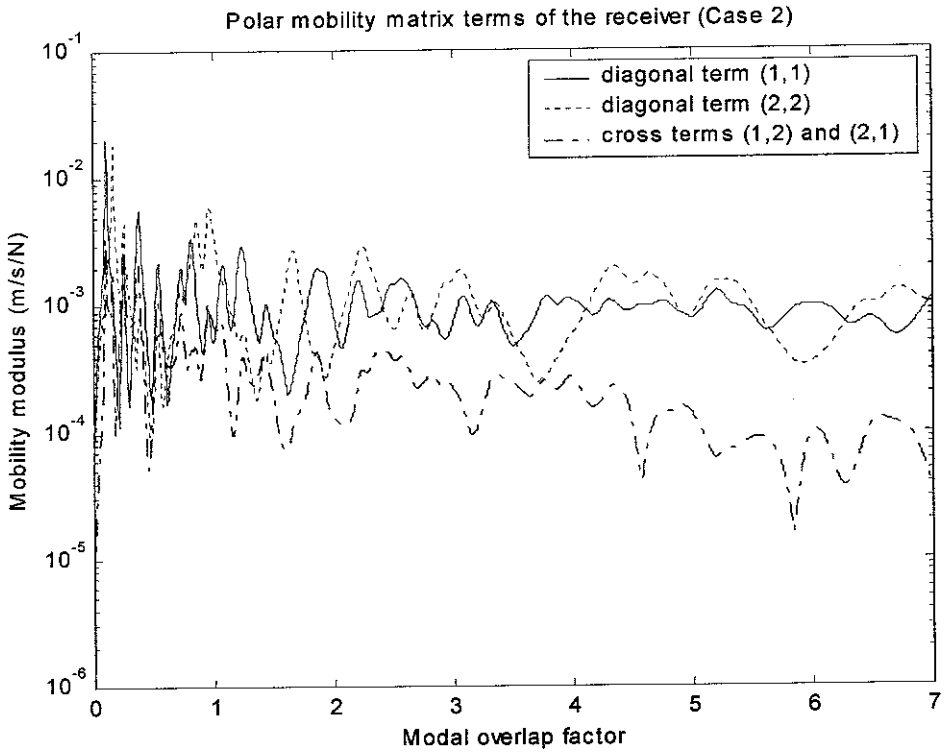

Figure 2.5

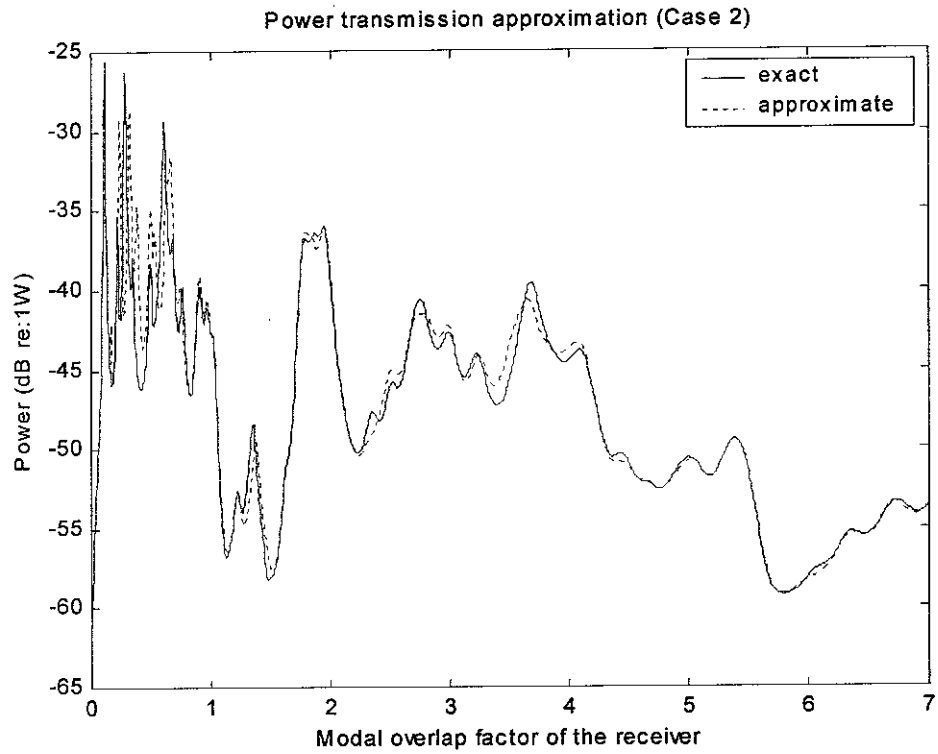

Figure 2.6

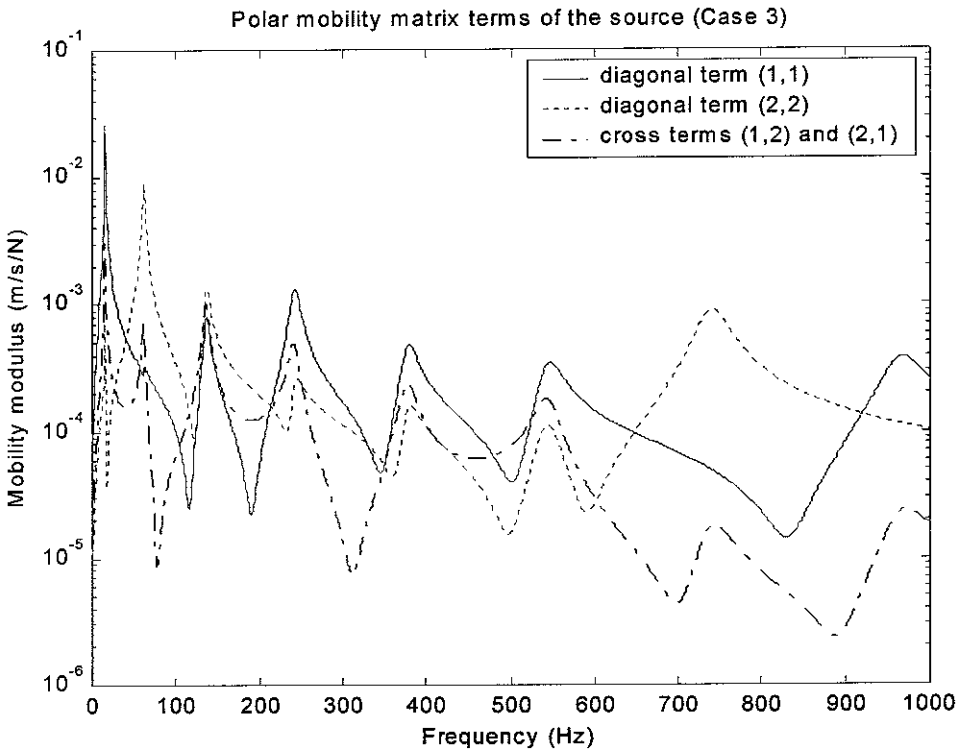

Figure 2.7

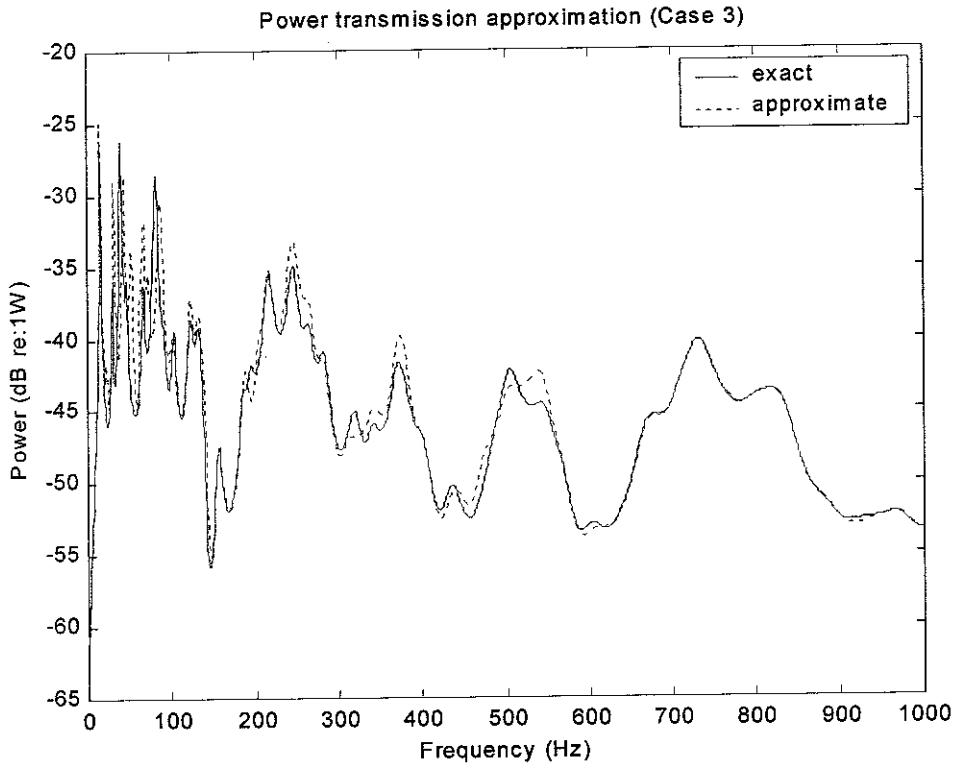
Power transmission approximation (Case 3)
exact
approximate
Power (dB re:1W)
-20
-25
-30
-35
-40
-45
-50
-55
-60
-65
0
100
200
300
400
500
600
700
800
900
1000
Frequency (Hz)

Figure 2.8

3. Power transmission through discrete couplings, Part II: Application of the power mode method

3.1 The power mode theory

In [16], a new technique, power mode method, was developed to simplify the prediction of the power transmitted to flexible receivers from discrete force/velocity sources. The method approximates the transmitted power by the mean value and upper and lower bounds. In summary the power mode approach is a transformation from physical to modal forces and responses, analogous to the multipole approach, but of a more general form so that the transformed mobility/impedance matrix becomes diagonal. Based on this power mode theory again, this study is an attempt to approximately and simply predict the vibrational power transmitted to a flexible receiver from discrete general linear sources, i.e., the power transmission from a stiff source structure to a flexible receiver structure by discrete point couplings. For convenience the main principles of power mode theory are recapitulated below. Further details are given in [16].

For a general receiver structure excited by discrete force sources, the time-averaged real power can be calculated by

$$P = \frac{1}{2}\mathbf{F}^H \,\mathrm{Re}[\mathbf{M}]\mathbf{F} \tag{3.1}$$

where $\mathbf{M}$ is the complex mobility matrix of the structure. By matrix theories [17-18], $\mathrm{Re}[\mathbf{M}]$ can be decomposed into the form

$$\mathrm{Re}[\mathbf{M}] = \mathbf{\Psi D \Psi}^T \tag{3.2}$$

where $\mathbf{D}$ is a real and non-negative diagonal matrix composed of all the eigenvalues of $\mathrm{Re}[\mathbf{M}]$, and $\mathbf{\Psi}$ the normalized orthogonal matrix composed of the corresponding eigenvectors (in columns) such that $\mathbf{\Psi\Psi}^T = 1$. Usually the eigenvalues are arranged in descending order so that

$$D_{11} \geq D_{22} \geq \ldots \geq D_{NN} \geq 0 \tag{3.3}$$

Let the force vector $\mathbf{F}$ be weighted by $\mathbf{\Psi}$ so to give a new set of power modal forces

$$\mathbf{Q} = \mathbf{\Psi}^T\mathbf{F} \tag{3.4}$$

The relation

$$\sum_{n=1}^{N}|Q_n|^2=\sum_{n=1}^{N}|F_n|^2 \tag{3.5}$$

exists. Combining Equations (3.1), (3.2) and (3.4), the transmitted power to the receiver can be re-written as

$$P=\frac{1}{2}\sum_{n=1}^{N}|Q_n|^2 D_{nn} \tag{3.6}$$

The above equation denotes that the vibration power input to a structure by N forces can be regarded as the power input by N independent power modes. The set of forces $\mathbf{F}$ is defined by a new set of power modal forces $\mathbf{Q}$, and the receiver by a set of power modal mobilities D_{nn}.

In principle, full knowledge of $\mathrm{Re}[\mathbf{M}]$ is required to determine its eigenproperties, so ostensibly there are no benefits. However benefits do arise because in a number of situations approximations and bounds can be found for the transmitted power.

From equations (3.3), (3.5) and (3.6) upper and lower bounds can be simply derived as

$$P_{up}=\frac{1}{2}\left(\sum_{n=1}^{N}|F_n|^2\right)D_{11} \tag{3.7}$$

$$P_{low}=\frac{1}{2}\left(\sum_{n=1}^{N}|F_n|^2\right)D_{NN} \tag{3.8}$$

The mean value of the transmitted power to the receiver when averaged over all the power modes can then be approximated in terms of the mean square force and the mean point mobility

$$\bar{P}=\frac{1}{2}\left(\sum_{n=1}^{N}|F_n|^2\right)\mathrm{Re}\left(\sum_{n=1}^{N}M_{nn}\Big/N\right) \tag{3.9}$$

3.2 Power transmission approximation by the power mode method

For a source/receiver system, the interface force vector $\mathbf{F}$ of the receiver, by equation (1.6), is written as

$$\mathbf{F}=\left(\mathbf{M}_{\mathrm{R}}+\mathbf{M}_{\mathrm{S}}\right)^{-1}\mathbf{V}_{\mathrm{sf}} \tag{3.10}$$

The power transmission from the source to the receiver is given in equation (1.8). Physically the maximum power transmission will occur when the source structure is rigid, i.e.,

$$\mathbf{M}_S = [0] \tag{3.11}$$

so that the excitation velocities are in effect applied to the receiver structure directly. The upper bound of the power transmission therefore can be approximated as

$$P_{up} = \frac{1}{2}\mathrm{Re}\left\{\mathbf{V}_{sf}{}^{H}\mathbf{M}_R{}^{-1}\mathbf{V}_{sf}\right\} \tag{3.12}$$

From equation (3.10), it follows that

$$\sum_{n=1}^{N}|F_n|^2 = \mathbf{V}_{sf}{}^{H}\left[\left(\mathbf{M}_R + \mathbf{M}_S\right)^{-1}\right]^{H}\left(\mathbf{M}_R + \mathbf{M}_S\right)^{-1}\mathbf{V}_{sf} \tag{3.13}$$

Equation (3.13) is a positive definite quadratic form, and hence its strict lower bound can be found using steps similar to those described in section 3.1.

If $\mathbf{M}_R + \mathbf{M}_S$ is decomposed as

$$\mathbf{M}_R + \mathbf{M}_S = \mathbf{\Phi}\mathbf{\Lambda}_{RS}\mathbf{\Phi}^{H} \tag{3.14}$$

where $\mathbf{\Lambda}_{RS}$ is a diagonal matrix and $\mathbf{\Phi}$ the corresponding unitary matrix, then equation (3.13) can be re-written as

$$\sum_{n=1}^{N}|F_n|^2 = \mathbf{U}_{sf}{}^{H}\left[\mathbf{\Lambda}_{RS}{}^{-1}\right]^{H}\mathbf{\Lambda}_{RS}{}^{-1}\mathbf{U}_{sf} \tag{3.15}$$

where

$$\mathbf{U}_{sf} = \mathbf{\Phi}^{H}\mathbf{V}_{sf} \tag{3.16}$$

Combining equations (3.15) and (3.16), it gives

$$\sum_{n=1}^{N}|F_n|^2 \geq \left(\sum_{n=1}^{N}|V_{sf,n}|^2\right)\frac{1}{\left|\lambda_{\max}^{RS}\right|^2} \tag{3.17}$$

Here $\left|\lambda_{\max}^{RS}\right|$ is the maximum magnitude of the diagonal elements of $\mathbf{\Lambda}_{RS}$. In [19], it is seen that

$$\left|\lambda_{\max}^{RS}\right| \leq \sqrt{\lambda_{\max}^{\mathbf{M}_R^H\mathbf{M}_R}} + \sqrt{\lambda_{\max}^{\mathbf{M}_S^H\mathbf{M}_S}} \tag{3.18}$$

where $\lambda_{\max}^{\mathbf{M}_R^H\mathbf{M}_R}$ and $\lambda_{\max}^{\mathbf{M}_S^H\mathbf{M}_S}$ represent the maximum eigenvalues of matrices $\mathbf{M}_R^H\mathbf{M}_R$ and $\mathbf{M}_S^H\mathbf{M}_S$, respectively, and where

$$\sqrt{\lambda_{\max}^{\mathbf{M}_R^H\mathbf{M}_R}} \le \max_n |M_{R,nn}| + \sqrt{\sum_{n\neq m}\sum |M_{R,nm}|^2} \tag{3.19}$$

$$\sqrt{\lambda_{\max}^{\mathbf{M}_S^H\mathbf{M}_S}} \le \max_n |M_{S,nn}| + \sqrt{\sum_{n\neq m}\sum |M_{S,nm}|^2} \tag{3.20}$$

Combining equations (3.8), (3.17)-(3.20), a strict lower bound of power can be obtained as

$$P_{low} = \frac{\frac{1}{2}\left(\sum_{n=1}^{N}|V_{sf,n}|^2\right)\lambda_{\min}^R}{\left(\max_n |M_{R,nn}| + \sqrt{\sum_{n\neq m}\sum |M_{R,nm}|^2} + \max_n |M_{S,nn}| + \sqrt{\sum_{n\neq m}\sum |M_{S,nm}|^2}\right)^2} \tag{3.21}$$

where $\lambda_{\min}^R$ is the minimum eigenvalue of the receiver mobility matrix $\mathrm{Re}[\mathbf{M}_R]$.

For a very flexible and/or heavily damped receiver, the point mobility tends to be much larger than the transfer mobility so that the points can be taken as 'uncoupled', i.e.,

$$\mathbf{\Lambda}_R \approx \mathbf{M}_R,\ \mathrm{Re}[\mathbf{\Lambda}_R] \approx \mathrm{Re}[\mathbf{M}_R] \tag{3.22}$$

Equation (3.18) then becomes

$$\begin{aligned} |\lambda_{\max}^{RS}| &\le \max_n |M_{R,nn}| + \max_n |M_{S,nn}| + \sqrt{\sum_{n\neq m}\sum |M_{S,nm}|^2} \\ &\le \max_n |M_{R,nn}| + \left(1+\sqrt{N(N-1)}\right)\max_n |M_{S,nn}| \end{aligned} \tag{3.23}$$

The bounds of the transmitted power then can be approximated by

$$P_{up} \approx \frac{1}{2}\sum_{n=1}^{N}|V_{sf,n}|^2\,\mathrm{Re}\left\{\frac{1}{M_{R,nn}}\right\} \tag{3.24}$$

$$P_{low} \approx \frac{1}{2}\left(\sum_{n=1}^{N}|V_{sf,n}|^2\right)\frac{\min_n\left\{\mathrm{Re}\left[M_{R,nn}\right]\right\}}{\left(\max_n |M_{R,nn}| + \left(1+\sqrt{N(N-1)}\right)\max_n |M_{S,nn}|\right)^2} \tag{3.25}$$

Note that these bounds depend only on the diagonal elements of the mobility matrices. These can often be estimated (to a good approximation) from the equivalent infinite system if the modal overlap is high.

Of course the practical usefulness of these upper and lower power bounds depends on the width of this band. It can be seen that the stiffer the source and/or the more flexible the receiver, the closer the values of upper and lower bounds, i.e., the more narrow the band. Specifically, if the source structure is much stiffer than the receiver structure so that

$$\max_n |M_{R,nn}| >> \left(1+\sqrt{N(N-1)}\right)\max_n |M_{S,nn}| \tag{3.26}$$

the upper and lower bounds are almost the same. Under such circumstances, the power therefore can be actually approximated by that transmitted by a set of free velocities $\mathbf{V}_{sf}$.

It is known that a finite structure may be approximated by an equivalent structure of infinite extent to give the frequency average level of the response. This is because the frequency average point mobility of a finite structure equals that of the equivalent infinite structure. For a stiff-source/flexible-receiver system, the lower bound of the transmitted power can be quite close to the 'exact' value of the transmitted power, since the band width formed by the upper and lower bounds can be rather narrow if the mismatching between the source and the receiver is big enough. It is therefore reasonable to expect that the power transmitted from a stiff source to a finite flexible receiver can be simply and accurately approximated by

$$P \approx \frac{1}{2}\left(\sum_{n=1}^{N}\left|V_{sf,n}\right|^2\right)\frac{\mathrm{Re}\left\{M_{R,nn}^{\infty}\right\}}{\left(\left|M_{R,nn}^{\infty}\right|+\left(1+\sqrt{N(N-1)}\right)\max_n\left|M_{S,nn}\right|\right)^2} \tag{3.27}$$

where, $M_{R,nn}^{\infty}$ corresponds to the point mobility of the equivalent infinite receiver. The bigger the mismatching between the source and the receiver, the more accurate this approximation expression is.

In the above sections, only the power transmission in the vertical degree of freedom has been considered, this usually being the most significant [20]. However, the power transmission by other components of motion, particularly bending moments, is also desirable. Under such circumstances, by assuming no cross-coupling between these components of motion, the power transmission due to bending moment excitations can be approximated by analogy with equation (3.27), in which the free velocity vector is composed of a set of rotation "velocities" and the mobility corresponds to the frequency response function between the bending moment excitation and the rotation velocity.

3.3 Numerical examples

Three expressions have been derived in the section 3.2 to approximate the transmitted power from a stiff source to a flexible receiver by its upper and lower bound approximations as well as its frequency average response approximation. To investigate the validity and accuracy of these approximation approach, a numerical case is set up consisting of a stiff beam connected to a flexible rectangular plate by four evenly spaced points with a unit point force acting on the source beam, as shown in Figure 3.1.

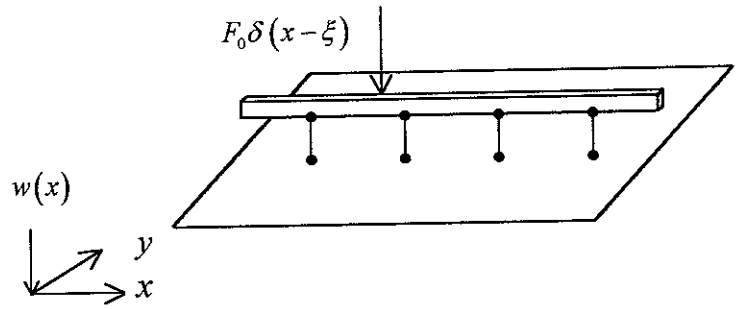

Figure 3.1 Point coupled beam-plate system

The boundary conditions of the beam and of the plate, the material of the system, as well as the external force excitation are all same as those in Section 2.3. Three different plate models, shown in Table 3.1, are used to investigate how the mismatching between the source and the receiver affect the accuracy of the approximations. It is seen then that the wavenumber ratios k_p/k_b are 2.5, 3.5 and 5.6 corresponding to the plate thickness 0.010m, 0.005m and 0.002m, respectively.

Table 3.1 Parameters of the beam and plate structures

Structure	Beam	Plate
Dimension sizes	Length=2m; width=0.059m; Height=0.068m	Length=2m; Width=0.9m; Thickness=0.010m/0.005m/0.002m

First the FRF-based sub-structuring technique is used to get the exact vibration responses of the coupled system, and then the approximations for the upper and lower bounds as well as the frequency average of the transmitted power are made using the expressions defined in equations (3.24), (3.25) and (3.27). The comparisons with the FRF results are shown in Figure 3.2-3.8. A running frequency average technique has been

used in the calculations to get the broad features of the transmitted power. The frequency-band used in the frequency average is chosen to be 10 Hz wide so that each band consists of a couple of (plate) vibration modes. (The plate modal densities are 0.15, 0.42 and 1.65 mode/Hz when the plate thickness is 0.010m, 0.005m and 0.002m, respectively.)

Figures 3.2-3.4 are the comparisons made between the approximated upper/lower bounds and the exact result of the transmitted power, corresponding to $k_p/k_b = 2.5$, 3.5 and 5.6, respectively. It can be seen that the band width formed by the approximated upper and lower bounds becomes more narrow as the plate receiver gets more flexible, as we have expected. It is easier to see from equation (3.25) that the more flexible the receiver is, the more accurate the lower bound approximation is. This trend, however, cannot be seen directly from the upper bound approximation expression of (3.12). Nevertheless, one can explain it using the general linear source properties, which has been briefly introduced in Section 1. The upper bound approximation is indeed made more broadly than the lower bound approximation, which gives the maximum available power transmission when the source only generates velocities at the interface DOFs, and therefore bigger errors can be caused between the exact results and the upper bound for a general linear source, see Figure 3.2, due to the source generated velocities at the interface DOFs are greatly effected by the generated interface forces. When the receiver becomes more flexible than the source, or the source mobility gets smaller than the receiver mobility, the source structure exhibits more velocity-source-like behaviour, i.e., the source generated velocities at the interface DOFs become less effected by the generated interface forces. Consequently, the upper bound approximations tend to be more accurate, as shown in Figure 3.3. When the receiver becomes much more flexible than the source structure, or the mobility of the source is much smaller than the mobility of the receiver, the source can almost be treated as a set of free velocity sources, i.e., the generated interface velocities are almost independent of the interface forces. As a result the transmitted power can then be simply approximated by that transmitted by a set of free velocities sources, as shown in Figure 3.4, especially for the frequency range where the modal overlap factor of the receiver is much greater than unity. It can be seen from Figure 3.5 that, in this case, the receiver is actually behaving in a "fuzzy" [13-14] manner, which is equivalent to add certain damping as well as mass to the vibrations of the source

structure. For the low modal overlap areas (of the receiver), say less than unity, neither the upper- or the lower-bound approximations are applicable.

Figures 3.6-3.8 are the frequency average approximations made using equation (3.27), corresponding to $k_p/k_b = 2.5$, 3.5 and 5.6, respectively. It can be seen that the frequency average power transmitted to the receiver can be accurately approximated provided the receiver has high modal overlap and is much more flexible than the source structure (e.g. the wavenumber of the receive is at least three or four times that of the source structure). When the receiver is not very flexible, see Figure 3.6, with a wavenumber ratio $k_p/k_b = 2.5$, the approximation tends to underestimates the frequency average value of the transmitted power about 3dB.

3.4 Summary

This study is an attempt to simplify the estimation of the transmitted power from a stiff source to a flexible receiver by discrete point coupling. Three new approximation expressions of power transmission have been derived using a new technique, the power mode method. The main results are summarized below:

(1) The maximum and minimum power transmission can be simply approximated by upper and lower power bounds. The practicality of these upper and lower power bounds depend on the width of this band. The bigger mismatch between the source and the receiver, the more narrow is this band.

(2) The frequency average power can be approximated quite accurately provided the receiver has high modal overlap and flexible enough compared to the source structure (e.g. the wavenumber of the receive is at least three or four times that of the source structure). In other cases, the approximation tends to underestimate the transmitted power.

(3) When the receiver structure is much more flexible than the source so that it behaves in a 'fuzzy' manner, the power can be regarded as transmitted mainly by a set of free velocities, especially for the mid- and high frequency ranges.

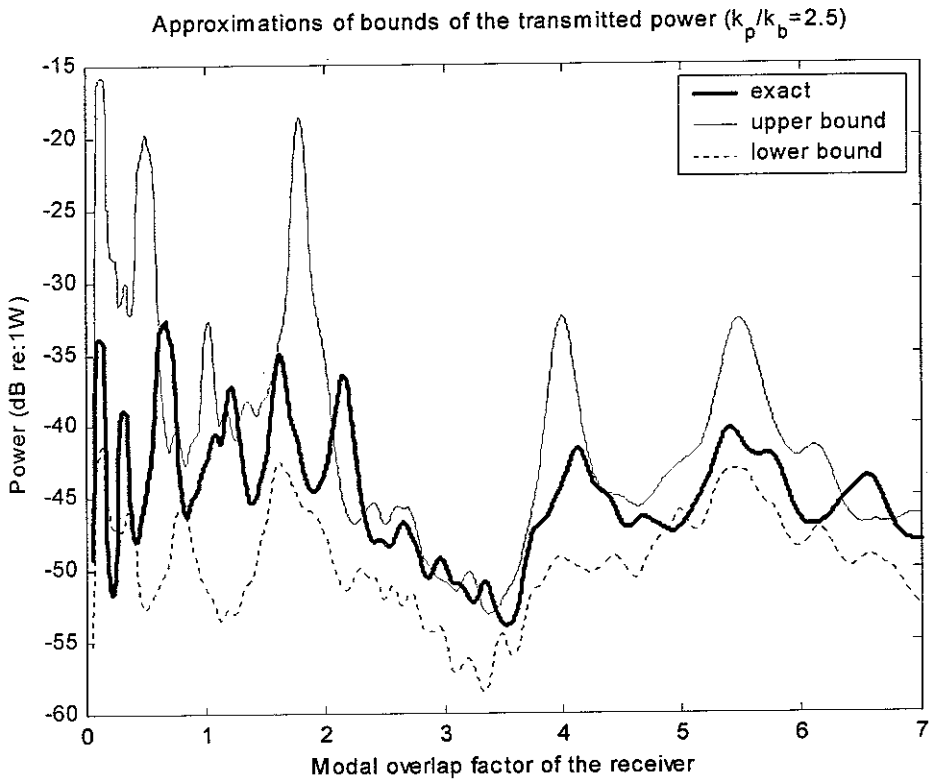

Figure 3.2

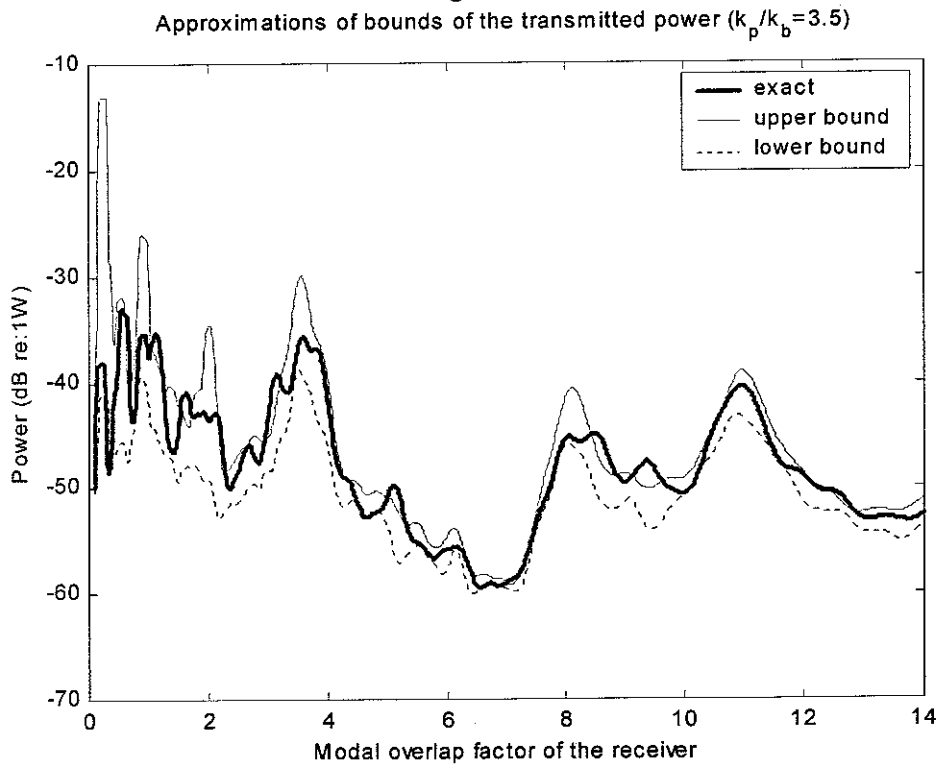

Figure 3.3

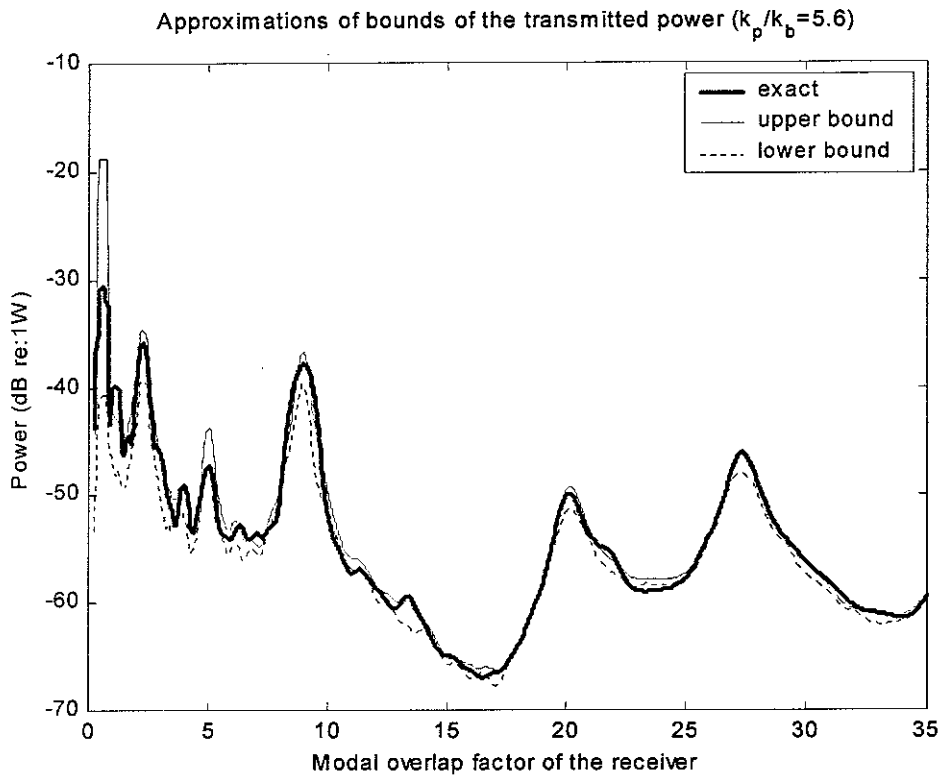

Figure 3.4

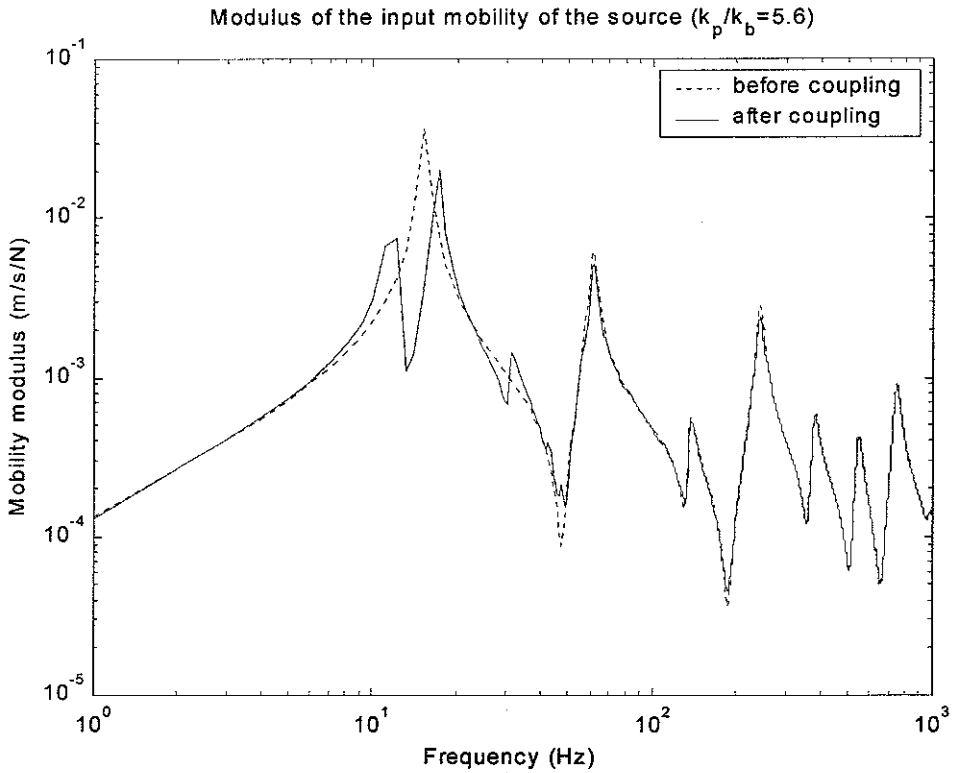

Figure 3.5

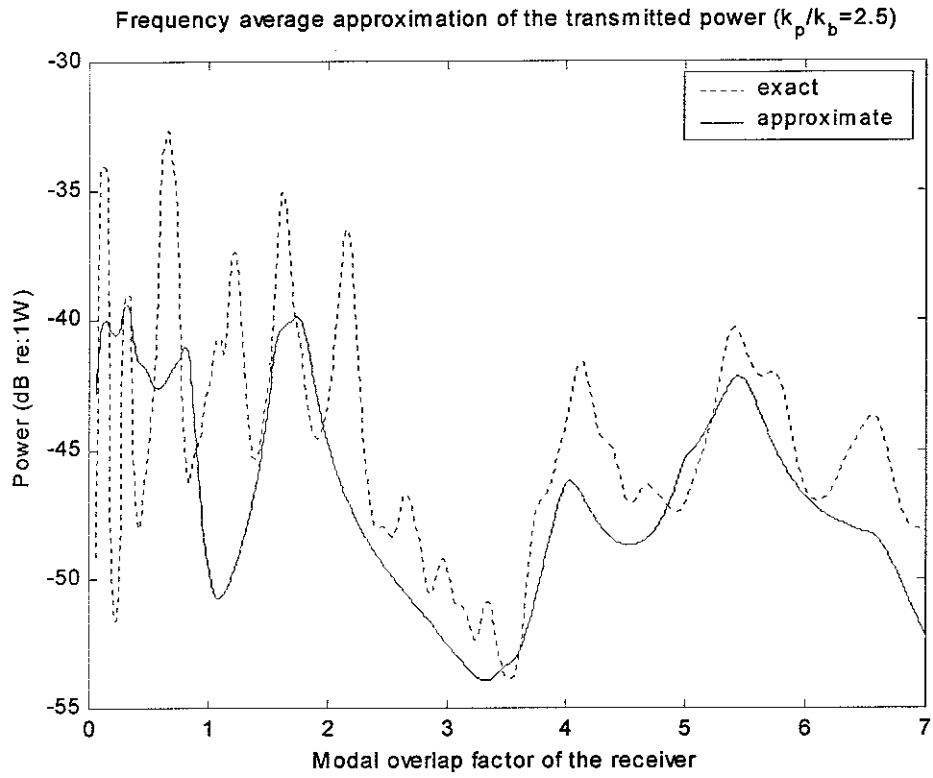

Figure 3.6

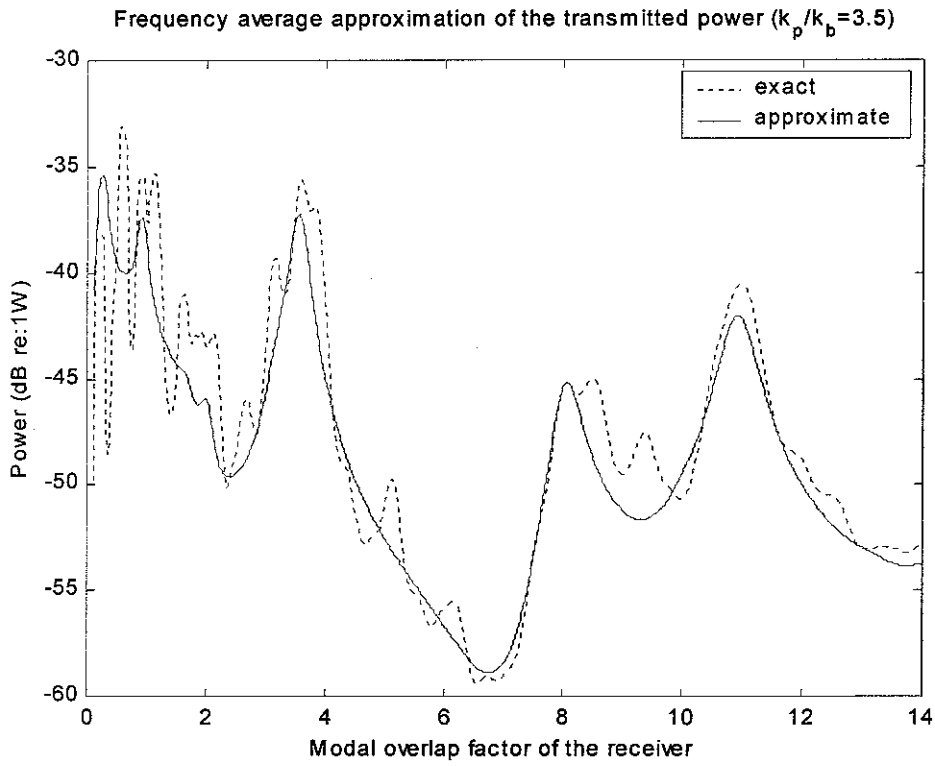

Figure 3.7

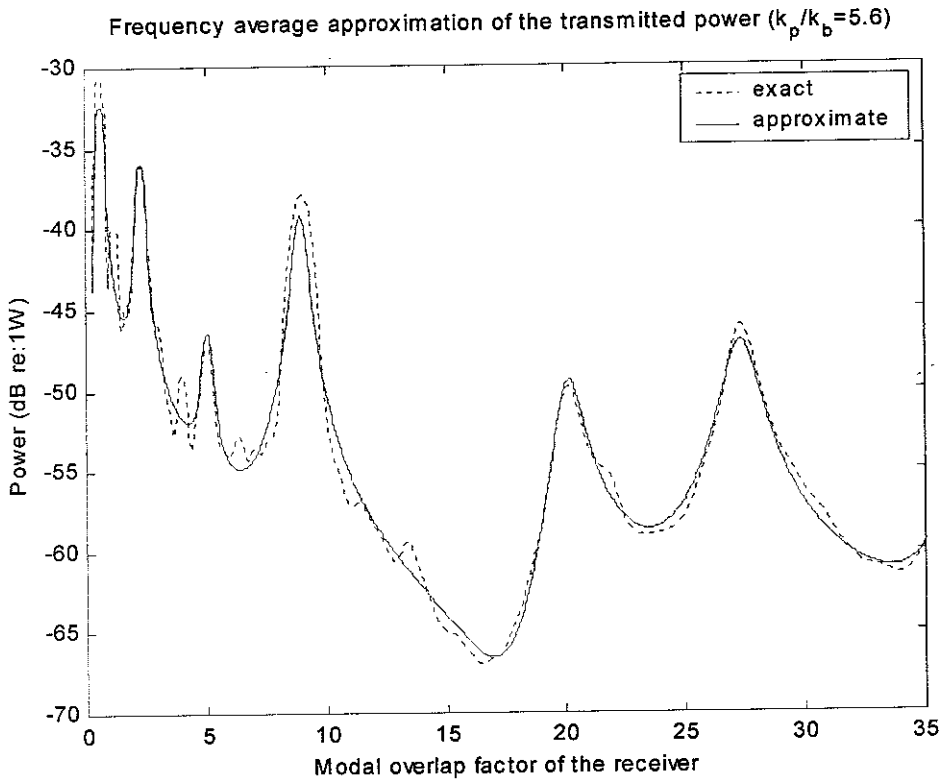
Frequency average approximation of the transmitted power (k_p/k_b=5.6)
exact
approximate
Power (dB re:1W)
-30
-35
-40
-45
-50
-55
-60
-65
-70
0
5
10
15
20
25
30
35
Modal overlap factor of the receiver

Figure 3.8

4. Power transmission through line couplings, Case 1: An infinite beam attached to an infinite plate

4.1 The Fourier Transform method

It has been shown in the companion Technical Memorandum [16] that the Fourier Transform method is particularly useful for predicting the power transmitted by a line-distributed source to an infinite uniform receiver. In this section this technique will be used to predict the power transmission between an infinite beam and an infinite plate.

In [22], the one-dimensional Fourier Transform is defined by

$$G(\beta)=\int_{-\infty}^{+\infty} g(x)e^{-j\beta x}dx \tag{4.1}$$

$$g(x)=\frac{1}{2\pi}\int_{-\infty}^{+\infty} G(\beta)e^{j\beta x}d\beta \tag{4.2}$$

For an infinite beam attached to an infinite plate with an external point force F_0 acting at $x=0$, if it is assumed that the beam drives the plate with a force distribution $f(x)$ along the coupling line, the equation of motion of the beam then can be written as

$$D_b\frac{\partial^4 w_b(x)}{\partial x^4}+m_b\frac{\partial^2 w_b(x)}{\partial t^2}=F_0\delta(x)-f(x) \tag{4.3}$$

Using equations (4.1) and (4.2), the beam equation can be written in the wavenumber domain as

$$D_b k^4 W_b(k)-m_b\omega^2 W_b(k)=F_0-F(k) \tag{4.4}$$

Thus both the displacement of the beam and the force distribution are transformed into the wavenumber domain. This will yield an algebraic equation for the dynamic response which can be solved analytically as below.

If $Z(k)$ represents the line (dynamic) stiffness of the plate to the beam (in the wavenumber domain), then

$$F(k)=Z(k)W_b(k) \tag{4.5}$$

where $Z(k)$ was derived in [16] as

$$Z(k)=2D_p\sqrt{k^4-k_p^4}\left(\sqrt{k^2+k_p^2}+\sqrt{k^2-k_p^2}\right) \tag{4.6}$$

and where $k_p=\sqrt{m_p\omega^2/D_p}$ is the wavenumber of the plate.

Combining equations (4.4), (4.5) and (4.6), the following relation can be derived

$$W_b(k)=\frac{F_0}{D_b k^4-m_b\omega^2+Z(k)} \tag{4.7}$$

The general expression for the power transmitted to the plate is written as

$$P=\frac{1}{2}\mathrm{Re}\left\{\int_{-\infty}^{+\infty} f^*(x)\,j\omega w_b(x)\,dx\right\} \tag{4.8}$$

From [22], equation (4.8) is equivalent to

$$P=\frac{1}{2}\mathrm{Re}\left\{\frac{1}{2\pi}\int_{-\infty}^{+\infty} F^*(k)\,j\omega W_b(k)\,dk\right\} \tag{4.9}$$

From equation (4.6) it can be seen that when $|k|\geq k_p$ then $\mathrm{Im}(Z)\approx 0$, neglecting the small damping of the plate. Hence equation (4.9) can be simplified as

$$P=\frac{\omega}{4\pi}\mathrm{Im}\left\{\int_{-k_p}^{+k_p} Z(k)\left|W_b(k)\right|^2 dk\right\} \tag{4.10}$$

Physically the above expression demonstrates that only the wave terms with $k<k_p$ can radiate power to the plate, and thus only the wave terms with wavenumber less than k_p should be taken into account to estimate the power transmission from the beam to the plate. A good simplification can then be made to predict the transmitted power in the wavenumber domain.

4.2 Wave analysis method

Similarly, the dynamic response of such a coupled beam/plate system can also be obtained by wave analysis method. In [11-12], the line impedance of the plate to the beam has been derived in terms of waves as

$$Z_p(k_b')=\frac{2m_p\omega}{k_p}\sqrt{1-\left(\frac{k_b'}{k_p}\right)^4}\left(\sqrt{1+\left(\frac{k_b'}{k_p}\right)^2}+j\sqrt{1-\left(\frac{k_b'}{k_p}\right)^2}\right) \tag{4.11}$$

where k_b' is the wavenumber of the beam after coupling. Multiplying $j\omega$ to both sides of equation (4.11), it is seen then that $j\omega Z_p(k_b')$ is formally identical to $Z(k)$ which is given in equation (4.6) derived from the Fourier Transform approach.

Usually the plate is relatively thin so that k_b'/k_p is less than unity. If $(k_b'/k_p)^2 << 1$, equation (4.11) can be approximated by

$$Z_p \approx \frac{2m_p\omega}{k_p}(1+j) \tag{4.12}$$

Equation (4.12) shows that provided the plate wavenumber is much larger than the coupled beam wavenumber, the line impedance of the plate is independent of the beam properties, and also the plate can be regarded as locally reacting [11-12]. Having determined the condition under which the plate can be considered locally reacting, it is appropriate to consider the dispersion relation for a beam coupled to a general locally reacting receiver plate. In this case, the general dispersion relation is given by [11]

$$D_b k_b'^4 = m_b\omega^2 - j\omega Z_p \tag{4.13}$$

Equation (4.13) shows that in effect the presence of the plate loads the dynamic response of the beam. Then the dynamic response as well as the power transmission of the coupled beam/plate system can be approximated simply.

Assume that the $F_0\delta(x)$ acted at the position of $x=0$ of the beam. Then before coupling with the plate, the displacement response at point x is defined as [8]

$$w_b(x) = \frac{F_0}{j4D_b k_b^3}\left(e^{-jk_b x} - je^{-k_b x}\right),\ x \geq 0 \tag{4.14}$$

$$w_b(x) = \frac{F_0}{j4D_b k_b^3}\left(e^{jk_b x} - je^{k_b x}\right),\ x < 0 \tag{4.15}$$

where $k_b = \sqrt[4]{m_b\omega^2/D_b}$ is the wavenumber of the uncoupled beam. After coupling the wavenumber of the beam becomes

$$k_b' = \sqrt[4]{\frac{m_b\omega^2 - j\omega Z_p}{D_b}} \tag{4.16}$$

The coupled response of the beam can then be approximated as

$$w_b(x) \approx \frac{F_0}{j4D_b k_b'^3}\left(e^{-jk_b'x} - je^{-k_b'x}\right),\ x \geq 0 \tag{4.17}$$

$$w_b(x) \approx \frac{F_0}{j4D_b k_b'^3}\left(e^{jk_b'x} - je^{k_b'x}\right),\ x < 0 \tag{4.18}$$

The transmitted power from the beam to the plate then can be approximated by

$$P \approx \frac{1}{2}\mathrm{Re}\left\{2\omega^2 \int_0^{+\infty} Z_p \left|w_b(x)\right|^2 dx\right\} \tag{4.19}$$

4.3 Discussion

The coupling effects of the plate on the beam can be obtained deterministically by the dynamic analysis of the beam/plate system in Section 4.1.

From equation (4.6), it follows that when $|k| < k_p$, then

$$Z(k) = \mathrm{Re}(Z) + j\,\mathrm{Im}(Z) \tag{4.20}$$

where

$$\mathrm{Re}(Z) = -2D_p\left(k_p^2 - k^2\right)\sqrt{k_p^2 + k^2} \tag{4.21}$$

$$\mathrm{Im}(Z) = 2D_p\left(k_p^2 + k^2\right)\sqrt{k_p^2 - k^2} \tag{4.22}$$

For simplicity, the small material loss factor of the plate η_p has been ignored. Equation (4.7) becomes

$$W_b(k) = \frac{F_0}{D_b k^4 - m_b\omega^2 + \mathrm{Re}\{Z(k)\} + j\,\mathrm{Im}\{Z(k)\}} \tag{4.23}$$

This equation can be rewritten as

$$W_b(k) = \frac{F_0}{D_b\left[1 + j\left(\eta_b + \eta_k\right)\right]k^4 - \left[m_b + m_k\right]\omega^2} \tag{4.24}$$

where

$$\eta_k = \frac{\mathrm{Im}(Z)}{D_b k^4} \tag{4.25}$$

$$m_k = -\frac{\mathrm{Re}(Z)}{\omega^2} \tag{4.26}$$

Thus the effect of the plate on the vibration of the beam can be regarded as to add damping η_k and a mass per unit length m_k to the beam. The energy dissipated by η_k represents the energy transmitted from the beam to the plate.

Substituting equations (4.21) and (4.22) into (4.25) and (4.28), respectively gives

$$\eta_k = \frac{2D_p\left(k_p^2+k^2\right)\sqrt{k_p^2-k^2}}{D_b k^4} \tag{4.27}$$

$$m_k = \frac{2D_p\left(k_p^2-k^2\right)\sqrt{k_p^2+k^2}}{\omega^2} \tag{4.28}$$

Equation (4.27) indicates that the damping effects of the plate on the beam depend on both the properties of the beam and of the plate regardless of the internal damping of the plate. Equation (4.28) denotes, however, that the mass added to the beam by the plate tends to depend on the plate properties only.

When $k << k_p$, these expressions reduce to

$$\eta_k \approx \frac{2D_p}{D_b k_p}\left(\frac{k_p}{k}\right)^4 \approx \frac{m_p}{m_p + m_b k_p/2} \tag{4.29}$$

$$m_k \approx \frac{2m_p}{k_p} = \frac{m_p \lambda_p}{\pi} \tag{4.30}$$

From equation (4.29) one may reasonablly suppose that when a set of wave travels along the beam, the waves with fast wave velocity (k is very small) can transmit most of their energy to the plate. Equation (4.30) shows that the mass added to the beam is almost equivalent to the plate mass in a strip of width equal to one third of the plate wavelength. When the plate receiver is much more flexible than the source beam (e.g. behaves in a "Fuzzy" manner to the beam), it is seen then the damping added on the beam depends on the wavenumber of the plate as well as the mass ratio between the beam and the plate only, regardless of the internal damping of the plate. This is in good agreement with the fuzzy structure theory [13-14].

For $|k| \geq k_p$, no damping is added to the beam by the plate since $\mathrm{Im}(Z) \approx 0$, i.e., waves travelling along the beam with wavenumber greater than the plate wavenumber will not

radiate power to the plate. In this situation, the influence of the plate on the beam vibrations can be regarded as mainly increasing its stiffness by D_k so that

$$W_b(k) = \frac{F_0}{(D_b + D_k)k^4 - m_b\omega^2} \tag{4.31}$$

where

$$D_k = \frac{2D_p}{k^4}\sqrt{k^4 - k_p^4}\left(\sqrt{k^2 + k_p^2} + \sqrt{k^2 - k_p^2}\right) \tag{4.32}$$

When $k >> k_p$, the added stiffness of the beam by the plate can be estimated by

$$D_k \approx \frac{4D_p}{k} = \frac{2D_p\lambda_b}{\pi} \tag{4.33}$$

Equation (4.33) means that the stiffness added to the beam is almost equivalent to the plate stiffness in a strip of width $2/\pi$ times the beam wavelength.

4.4 Numerical examples

In Section 4.1, an analytical solution of the power transmission has been given in the wavenumber domain as equation (4.7). Moreover in Section 4.2 it was seen that if the plate receiver is so flexible that $\left(k_p/k_b\right)^2 >> 1$, the plate can be regarded as locally reacting, as shown in equation (4.12). Consequently, the power transmitted within the beam/plate system can be approximated simply by equation (4.19). A numerical model is therefore set up to investigate how the wavenumber ratio k_p/k_b affects the accuracy of the locally reacting approximation, comprising an infinite beam attached to an infinite plate with an external point force acts on the beam at the point $x = 0$. Three different wavenumber ratios are investigated for which three different thickness of the plate are chosen. All the relevant parameters are listed in Table 4.1.

Table 4.1 Parameters of the numerical beam and plate structures

Structure	Beam	Plate
Dimension sizes	Width=0.059m; Height=0.068m	Thickness=0.020m/0.010m/0.005m
Material properties	Young's modulus=4.4e9 N/m^2; Density=1152kg/m^3; Loss factor=0.05; Poisson's ratio=0.38	

It is seen then that $k_p/k_b = 1.8$, 2.5, and 3.5 corresponding to the plate thickness 0.020m, 0.010m and 0.005m, respectively.

Firstly the input mobilities of the beam before and after coupling with the plate are predicted by the analytical FT approach. Then the input mobility of the beam after coupling is simply approximated by the locally reactive theory. Comparisons are made in Figures 4.1-4.3 for $k_p/k_b = 1.8$, 2.5 and 3.5, respectively. It can be seen the modulus of the input mobility of the beam, after coupling with the plate, decreases in a manner which can be explained well as the beam being loading more mass and damping by the presence of the plate. It also can be seen that the input mobility of the coupled beam tends to be less affected as the plate flexibility increases. This means the coupling effects between the beam and the plate decrease when the plate receiver is more flexible. All these three figures have shown that the locally reacting approximation gives a good estimate of the input mobility of the coupled beam, even when $k_p/k_b = 1.8$. In [11], the locally reacting theory is considered to be valid when $k_p/k_b \geq 2$.

Then Figures 4.4-4.6 show the comparisons of the transmitted power using the analytical prediction of equation (4.7) and the approximate result of equation (4.19). It can be seen that the locally reacting approximation agrees well with the analytical result, provided the plate wavenumber is at least twice that of the beam.

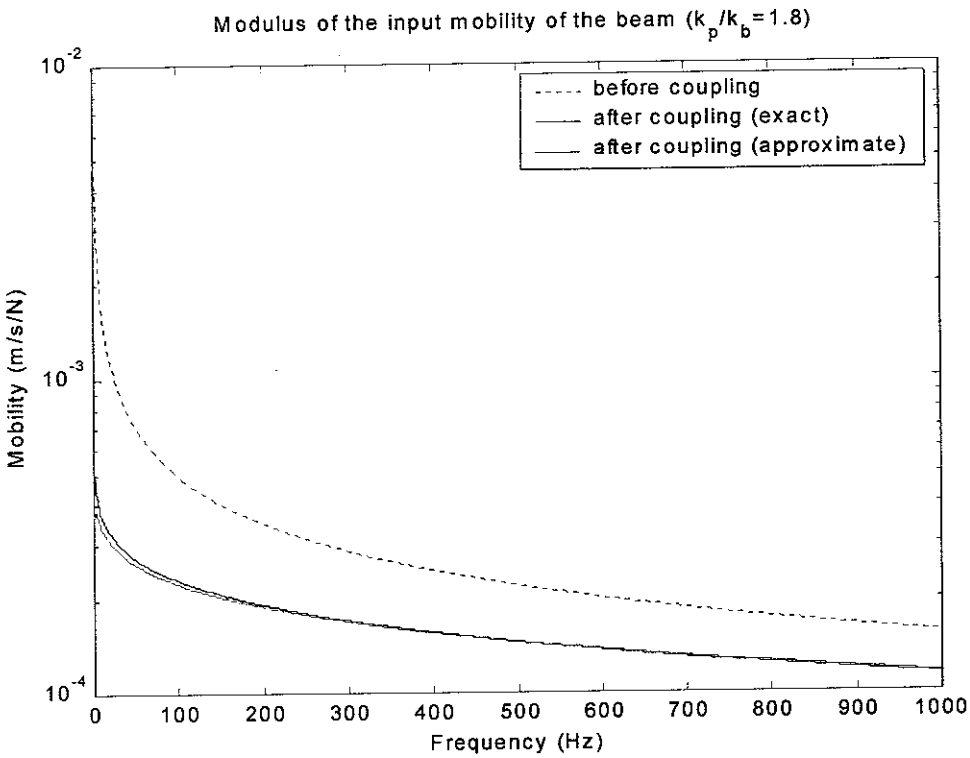

Figure 4.1

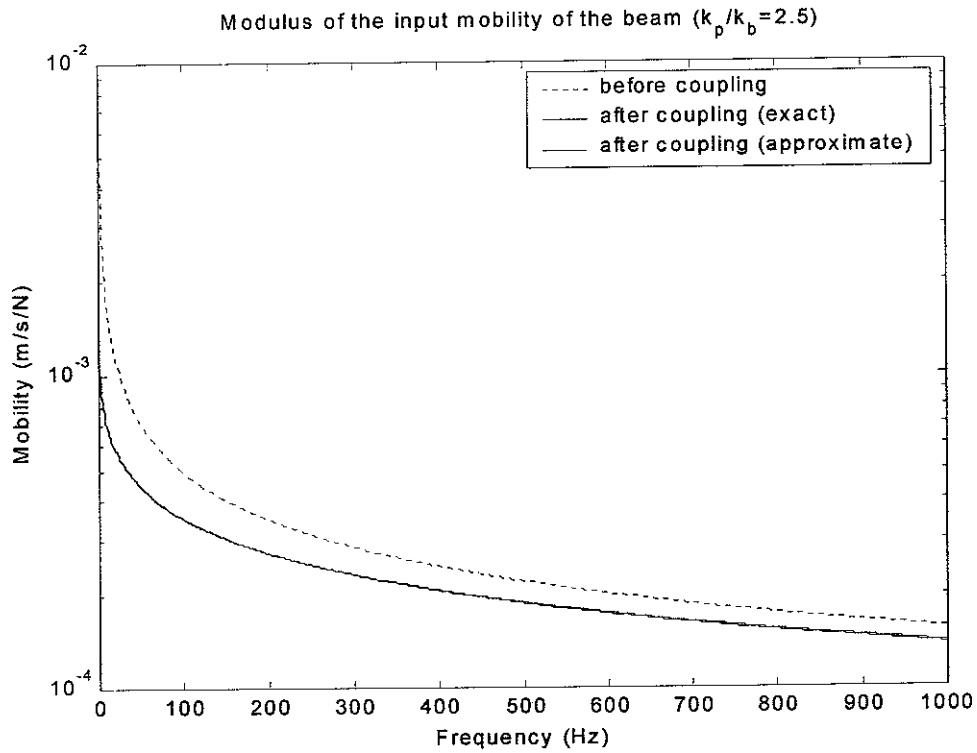

Figure 4.2

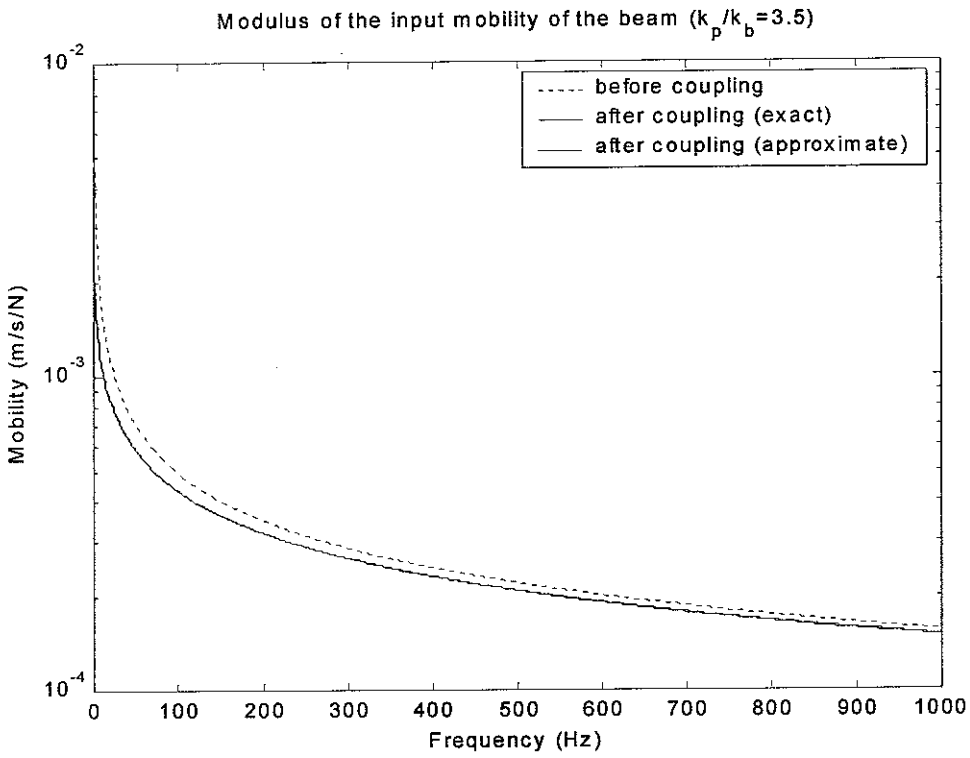

Figure 4.3

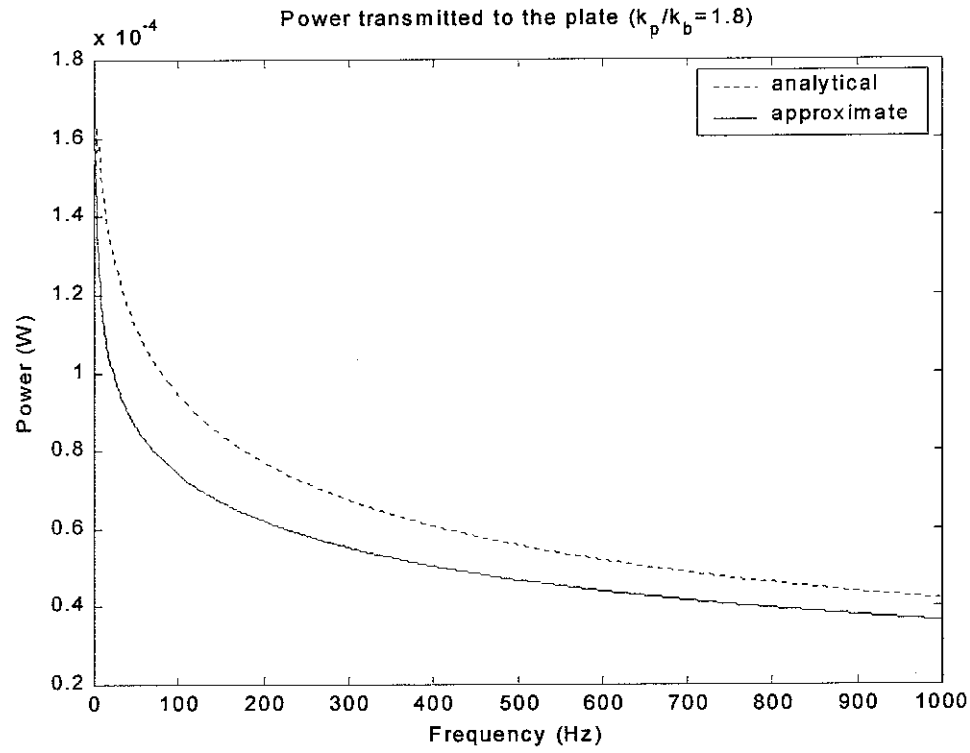

Figure 4.4

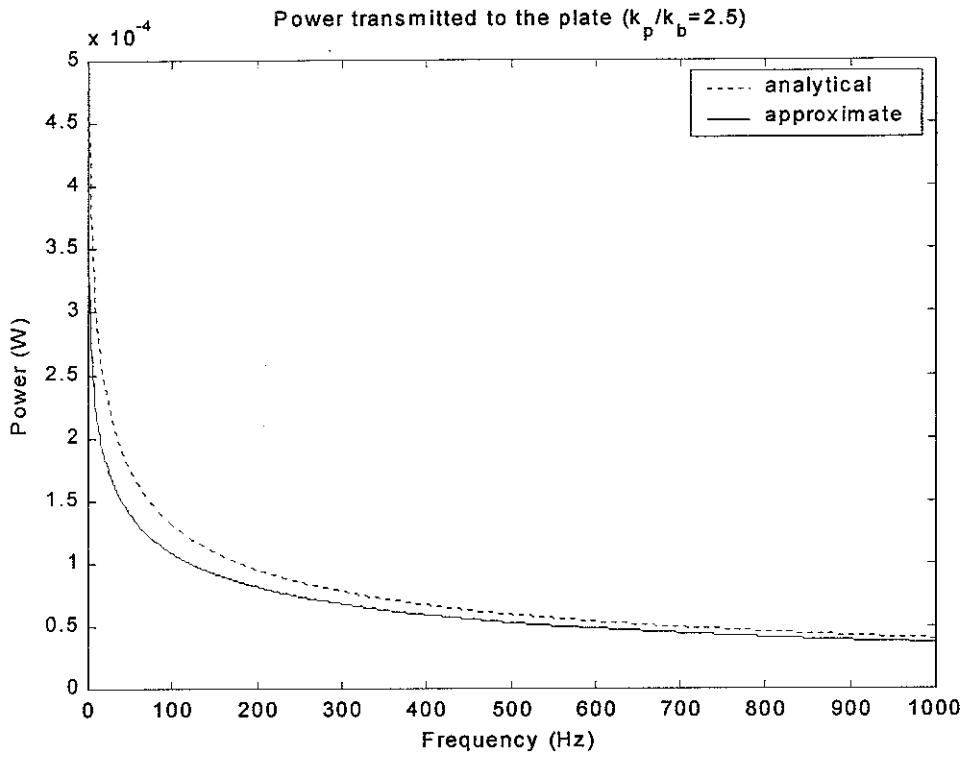

Figure 4.5

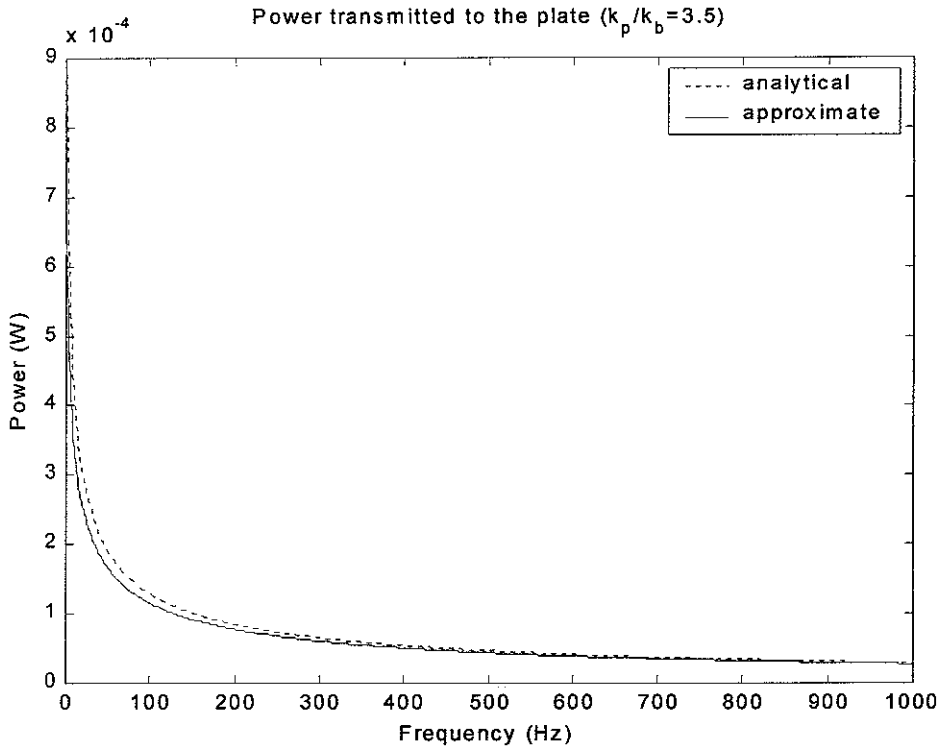

Figure 4.6

5. Power transmission through line couplings, Case 2: A finite beam attached to an infinite plate

5.1 Dynamic analysis by a combined modal analysis/Fourier Transform method

In the companion study [16], it has been shown that for line-distributed force sources modal analysis and Fourier Transform methods can be used to predict the transmitted power to the flexible receiver in a straightforward way. In Section 4.1 an analytical expression of the power transmission from an infinite source beam to an infinite thin receiver plate through line coupling, is derived based on the Fourier Transform approach. If the source beam of the coupled system is finite and its vibration exhibits obvious resonant behaviour, however, this FT-based approach is not applicable any more. In this section, a new approach which combines modal analysis and Fourier Transform methods is then developed to simply and accurately predict the power transmitted to an infinite plate from a finite source beam. The procedure is described below.

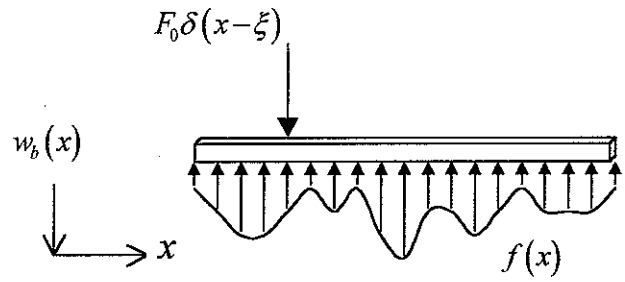

Figure 5.1 A finite beam excited by a point force and a distributed force

Suppose a finite beam structure is excited simultaneously by a point force $F_0\delta(x-\xi)$ and by a distributed force $f(x)$, as shown in Figure 5.1. The displacements along the beam length can then be expressed in a general form of

$$w_b(x) = F_0 Y_b(x,\xi) - \int_0^{L_b} f(x_0) Y_b(x,x_0)\, dx_0 \tag{5.1}$$

where L_b is the beam length, and $Y_b(x,x_0)$ is the transfer receptance or the Green function of the beam. The receptance can be written in terms of the uncoupled modes of the beam as

$$Y_b(x,x_0)=\sum_m b_m\phi_m(x)\phi_m(x_0) \tag{5.2}$$

where $\phi_m(x)$ is the m th mass normalized mode shape of the beam,

$$b_m=\frac{1}{\omega_m^2(1+j\eta_m)-\omega^2} \tag{5.3}$$

and η_m is the material loss factor of the beam corresponding to the m th mode. The displacement of the beam, therefore, can be written in the form

$$w_b(x)=\sum_n w_n\phi_n(x) \tag{5.4}$$

Now let $f(x)$ represent the interface force applied to the beam by the plate along the coupling, and also decompose $f(x)$ into components of these beam modes so that

$$f(x)=\sum_n f_n\phi_n(x) \tag{5.5}$$

From equations (5.1) and (5.5), it follows that

$$\sum_n w_n\phi_n(x)=F_0\sum_m b_m\phi_m(x)\phi_m(\xi)-\int_0^{L_b}\left(\sum_n f_n\phi_n(x_0)\right)\left(\sum_m b_m\phi_m(x)\phi_m(x_0)\right)dx_0 \tag{5.6}$$

Multiplying both sides of the above equation by $\phi_n(x)$ and integrating along the beam length, it is found that

$$w_n=F_0 b_n\phi_n(\xi)-\frac{b_n f_n}{m_b} \tag{5.7}$$

where m_b is the mass per unit length of the beam.

Equation (5.7) shows that the effect of the plate is to apply additional forces to each mode of the beam, thus affecting the response in that mode. The next stage is therefore to use the Fourier Transform approach to estimate the added modal forces.

The Fourier Transforms of the components of the beam displacement and of the interface force, due to the n th mode $\phi_n(x)$ of the beam, have the forms

$$W_{b,n}(\beta)=w_n\int_0^{L_b}\phi_n(x)e^{-j\beta x}dx=w_n\Phi_n(\beta) \tag{5.8}$$

$$F_n(\beta)=f_n\int_0^{L_b}\phi_n(x)e^{-j\beta x}dx=f_n\Phi_n(\beta) \tag{5.9}$$

It was seen in Section 4.1 that the Fourier Transformed line dynamic stiffness of an infinite plate is

$$Z(\beta)=2D_p\sqrt{\beta^4-k_p^4}\left(\sqrt{\beta^2+k_p^2}+\sqrt{\beta^2-k_p^2}\right) \tag{5.10}$$

An approximation is now introduced by assuming that the displacements of the plate outside the coupling joint with the beam can be ignored, i.e., by approximating the plate response along $y=0$ as

$$w_p(x)=\begin{cases} w_b(x), & (0\le x\le L_b) \\ 0, & (x<0)\cup(x>L_b) \end{cases} \tag{5.11}$$

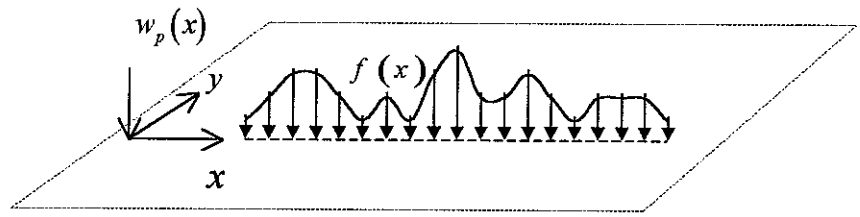

Figure 5.2 An infinite plate excited by a distributed force

Then

$$\sum_n f_n\Phi_n(\beta)=Z(\beta)\sum_n w_n\Phi_n(\beta) \tag{5.12}$$

By Fourier Transform theory it is known that

$$\int_0^{L_b}\phi_n(x)\phi_m(x)dx=\frac{1}{2\pi}\int_{-\infty}^{+\infty}\Phi_n^*(\beta)\Phi_m(\beta)d\beta=\begin{cases} 1/m_b, & n=m \\ 0, & n\ne m \end{cases} \tag{5.13}$$

Multiplying both sides of equation (5.12) by $\widetilde{\Phi}_n^*(\beta)$ and integrating over β from $-\infty$ to $+\infty$, it follows that

$$f_n=\left[\frac{1}{2\pi}\int_{-\infty}^{+\infty}m_b\left|\Phi_n(\beta)\right|^2Z(\beta)d\beta\right]w_n=Z_nw_n \tag{5.14}$$

where Z_n represnents the dynamic stiffness of the nth mode. Substituting equation (5.14) into (5.7) gives

$$w_n=\frac{b_n}{1+b_nZ_n/m_b}F_0\phi_n(\xi) \tag{5.15}$$

The power transmission from the beam to the plate can be expressed as

$$P=\frac{1}{2}\mathrm{Re}\left\{\sum_n\int_0^{L_b}\left[f_n\phi_n(x)\right]^* j\omega\left[w_n\phi_n(x)\right]dx\right\}=\frac{1}{2}\left(\frac{\omega}{m_b}\sum_n|w_n|^2\,\mathrm{Im}\{Z_n\}\right) \quad (5.16)$$

Equation (5.16) can be re-expressed in the wavenumber domain as

$$P=\frac{1}{4\pi}\omega\sum_n|w_n|^2\,\mathrm{Im}\left\{\int_{-\infty}^{+\infty}\left|\Phi_n(\beta)\right|^2 Z(\beta)d\beta\right\} \quad (5.17)$$

From equation (5.10) it can be seen that $\mathrm{Im}\{Z(\beta)\}\approx 0$ when $|\beta|>k_p$ (ignoring the small damping of the plate). Thus equation (5.17) can be simplified to

$$P=\frac{1}{4\pi}\omega\sum_n|w_n|^2\,\mathrm{Im}\left\{\int_{-k_p}^{k_p}\left|\Phi_n(\beta)\right|^2 Z(\beta)d\beta\right\} \quad (5.18)$$

Physically, equation (5.18) denotes that only the components of the beam response with wavelengths greater than the plate wavelength can transmit power to the plate, while the short wavelength components cannot transmit power. This is in agreement with the case of an infinite beam attached to an infinite plate. Thus it is reasonable to suppose that the wave components of the source beam with wavelengths shorter than the plate wavelength cause only near-field wave motions of the plate, or one may say that the plate can 'block' the short wavelength wave motions of the beam. As a result great simplifications to approximate the coupled responses can be made by ignoring all the short wave terms but with very good accuracy.

5.2 The locally reacting impedance method

In Section 4.2, it was seen that the plate can be regarded as locally reacting, provided the plate wavenumber is at least twice that of the coupled beam. Therefore it is possible to approximate the power transmission of a stiff source/flexible receiver system, where $k_b'/k_p<0.5$, by the locally reacting impedance method.

The locally reacting impedance of the plate has been approximated in equation (4.13) as

$$Z_p\approx\frac{2m_p\omega}{k_p}(1+j) \quad (5.19)$$

Then the interface force $f(x)$ applied to the plate by the beam along the coupling can be expressed as

$$f(x)=j\omega w_p(x)Z_p \quad (5.20)$$

The beam displacement of equation (5.6) becomes

$$w_b(x) = F_0 \sum_n b_n \phi_n(x) \phi_n(\xi) - \int_0^{L_b} \left(j\omega w_p(x_0) Z_p \right) \left(\sum_n b_n \phi_n(x) \phi_n(x_0) \right) dx_0 \qquad (5.21)$$

By the compatibility condition at the interface, it follows that

$$w_p(x) = w_b(x) = \sum_n w_n \phi_n(x) \qquad (5.22)$$

Equation (5.22) then, after some manipulation, can be written as

$$\sum_n w_n \phi_n(x) = F_0 \sum_n b_n \phi_n(x) \phi_n(\xi) - \sum_n b_n \left(\frac{j\omega w_n Z_p}{m_b} \right) \phi_n(x) \qquad (5.23)$$

Multiplying both sides of the above equation by $\phi_n(x)$ and integrating along the beam length gives

$$w_n = \frac{F_0 \phi_n(\xi)}{\omega_n^2 (1 + j\eta_b) - \omega^2 + \frac{j\omega Z_p}{m_b}} \qquad (5.24)$$

Comparing equations (5.15) and (5.24), it can be found that $Z_n \approx j\omega Z_p$ when a beam attached to a locally reacting plate, which only depends on k_p and m_p. The displacement of the interface can then be written as

$$w_p(x) = \sum_n \frac{F_0 \phi_n(\xi) \phi_n(x)}{\omega_n^2 (1 + j\eta_b) - \omega^2 + \frac{j\omega Z_p}{m_b}} \qquad (5.25)$$

Consequently the power transmitted can be approximated by

$$P = \frac{1}{2} \omega^2 \, \mathrm{Re} \left\{ Z_p \int_0^{L_b} |w_p(x)|^2 \, dx \right\} \qquad (5.26)$$

Equation (5.26) is derived based on the locally reacting impedance technique, i.e., the receiver is much more flexible than the source so that the correlations among the different points of the receiver (along the coupling) can be ignored. If it is not the case, e.g. the receiver is very stiff, the locally reacting theory will not hold, i.e., the correlations of the plate vibration at different points become significant. Equation (5.26) then cannot be used to provide a good approximation of the transmitted power. Equation (5.16) predicts the power by decomposing the interface dynamic responses (both displacement and force)

into the components of the beam modes so that the correlations among different components can always be ignored, due to the orthogonal property of modal shape functions. Therefore a very good approximation can be made to the transmitted power using equation (5.16), provided the only assumption concerning this combined mode/FT method holds, i.e., the displacement of the plate outside the coupling line with the beam can be ignored, regardless of the stiffness of the beam and/or the flexibility of the plate.

5.3 The effects of coupling the plate to the beam

In the above sections, the dynamic response and the transmitted power of the coupled beam/plate system are simply approximated based on a combined modal analysis/Fourier Transform method as well as locally reactive theory. Furthermore, a quantitative analysis of the coupling effects of the plate on the beam vibration can be described as below from Section 5.1.

For the finite beam excited by a point force $F_0\delta(x-\xi)$, its displacement before the coupling can be determined by

$$w_b(x)=\sum_n w_n\phi_n(x) \tag{5.27}$$

where

$$w_n = b_n F_0 \phi_n(\xi) \tag{5.28}$$

After coupling the expression of (5.28) becomes

$$w_n = b_n' F_0 \phi_n(\xi) \tag{5.29}$$

where

$$b_n' = \frac{b_n}{1+b_n Z_n/m_b} \tag{5.30}$$

Let equation (5.3) be re-expressed as

$$b_n = \frac{m_b}{D_b k_n^4(1+j\eta_n)-m_b\omega^2} \tag{5.31}$$

where $k_n = \sqrt[4]{m\omega_n^2/D_b}$ corresponds to the wavenumber of the beam at its nth natural frequency ω_n. Then equation (5.30) becomes

$$b_n' = \frac{m_b}{D_b k_n^4 (1 + j\eta_n) - m_b \omega^2 + Z_n} \tag{5.32}$$

The analysis in Section 5.1 has shown that only the long wave components are of interest for the coupled response. Thus the expression for Z_n in equation (5.14) can be approximated by

$$Z_n = \frac{1}{2\pi} \int_{-k_p}^{+k_p} m_b \left|\Phi_n(\beta)\right|^2 Z(\beta) d\beta \tag{5.33}$$

where

$$Z(\beta) = -2D_p \left(k_p^2 - \beta^2\right) \sqrt{k_p^2 + \beta^2} + j2D_p \left(k_p^2 + \beta^2\right) \sqrt{k_p^2 - \beta^2} \tag{5.34}$$

Then equation (5.32) may be re-expressed as

$$b_n' = \frac{m_b}{D_b k_n^4 \left[1 + j\left(\eta_n + \eta_n'\right)\right] - \left(m_b + m_n'\right)\omega^2} \tag{5.35}$$

where

$$\eta_n' = \frac{D_p}{\pi D_b k_n^4} \int_{-k_p}^{k_p} m_b \left|\Phi_n(\beta)\right|^2 \left(k_p^2 + \beta^2\right) \sqrt{k_p^2 - \beta^2}\, d\beta \tag{5.36}$$

$$m_n' = \frac{D_p}{\pi \omega^2} \int_{-k_p}^{k_p} m_b \left|\Phi_n(\beta)\right|^2 \left(k_p^2 - \beta^2\right) \sqrt{k_p^2 + \beta^2}\, d\beta \tag{5.37}$$

Thus the coupling effects of the plate on the beam can be regarded mainly as adding mass and damping to each vibration mode of the beam as given by equations (5.36) and (5.37). The energy dissipated by the added damping corresponds the energy transmitted from the beam to the plate. It also can be seen that the added damping depends on both the properties of the beam and of the plate, but is almost regardless of the internal damping of the plate, which is in good agreement with the result obtained from fuzzy theory [13-14]. The added mass only depends on the properties of the plate as well as the mode shape functions of the source beam. As frequency increases, the added mass tends to depend on the plate properties only.

5.4 Numerical examples

Numerical examples of a finite beam attached to an infinite plate are presented to investigate the validity of the combined mode/FT approximation method. For simplicity,

both the ends of the beam are chosen to be simply supported so that its nth mass normalized modal shape function is

$$\phi_n(x) = \sqrt{\frac{2}{m_b L_b}} \sin \frac{n\pi x}{L_b} \tag{5.38}$$

The same material, perspex, is used in the numerical model as in the previous sections. An external point force acts on the beam at a position which has a distance of $\xi = 0.73m$ from one end of the beam. All the other relevant parameters are listed in Table 5.1.

Table 5.1 Parameters of the numerical beam and plate structures

Structure	Beam	Plate
Dimension sizes	Length=2m; Width=0.059m; Height=0.068m	Thickness=0.020/0.010m/0.005m

First the FRF-based sub-structuring method is used, where the line coupling is modelled by many discrete point couplings. The infinite number of degrees of freedom along the coupling is replaced by a finite number of points. If the number of the points is big enough, an accurate prediction of the dynamic response of the coupled system can be obtained. Of course, the more points used, the more calculations are required. Therefore for a line coupling cases, the FRF-based sub-structuring method tends to be computationally prohibitive. Nevertheless, this approach can be used as a benchmark for evaluating the efficiency and accuracy of the approximations developed in this section.

Tests were conducted to ensure the approach converged. Figures 5.3-5.5 show the calculated results for the transmitted power when different number of points (per plate wavelength) are used in modelling the line coupling, corresponding to the three different plate thicknesses. These examples show that, provided the discrete points are spaced at no more than a quarter of the plate wavelength apart discrete point couplings can be used to accurately model the line coupling. Therefore, in the following evaluations, the exact power transmissions are calculated using the FRF-based sub-structuring method by modelling the line coupling as discrete point couplings spaced at a quarter of the plate wavelength.

The dynamic response of the beam is approximated using the combined mode/FT approach given by equation (5.15). Figures 5.6-5.8 show the approximate and exact input

mobility of the beam after coupling with plates of various thicknesses. It is seen that the dynamic response of the beam can be approximated quite accurately using the developed mode/FT approach, except in the low frequency area of Figure 5.6 which corresponds to the thickest plate. This is because in the low frequency area, both the beam and the plate wavelengths are very long, thus the plate displacements outside the coupling region are comparable with those of the coupling positions, while the approximation method developed here has ignored these displacements. But for mid- and high-frequency range, a very good approximation can be made using equation (5.15), even when the receiver is not very flexible compared to the source structure. When the plate receiver is flexible enough, see Figures 5.7-5.8, good approximations can be made for almost the whole frequency range, i.e., equation (5.11) on which this mode/FT approach based, always holds to good accuracy. Therefore, the more flexible the receiver, the more accurate the mode/FT approach.

Of course the most interest of this study is to approximate the power transmitted to the flexible receiver, which is given by equation (5.18). Comparisons between the approximate and the exact results are shown in Figures 5.9-5.11 for plate thicknesses of 0.020m, 0.010m and 0.005m, respectively. It can be seen that the approximations meet well with the exact results but are found with much less computational cost. For example, when the plate thickness is chosen to be 0.005m, the calculation time used by the mode/FT approximation approach only takes about one twentieth of that of the FRF-based sub-structuring method.

In Section 5.2 it is seen that the power transmission can also be approximated using equation (5.26) when the receiver structure is locally reactive, i.e., the receiver is very flexible so that the cross coupling between different points along the coupling can be ignored. Comparisons between this locally reactive approximation by equation (5.26) and the exact FRF predictions are made in Figures 5.12-5.14 for different plate receivers. It can be seen that the locally reacting impedance method can be quite accurate and efficient for approximating the power transmitted to the receiver. However, when equation (5.25) is used to approximate the input mobility of the coupled beam, as shown in Figures 5.15-5.17, it can be seen that this locally reacting approach is not applicable for predicting the dynamic response of the source structure, even when the receiver is

much more flexible than the source as shown in Figure 5.17. Nevertheless, as far as the transmitted power is concerned, the locally reacting impedance method is a good approach for a coupled system where the wavenumber of the receiver is at least twice that of the coupled source structure.

The final part of this numerical study concerns the coupling effects of the plate on the beam. Figure 5.18 shows the input mobilities of the source beam before and after coupling calculated using the FRF-based sub-structuring approach for various plate thickness. It can be seen that in effect the coupling effects of the plate on the beam can be regarded as adding damping and mass: the added mass decreases the lower natural frequencies of the beam significantly and the added damping decreases its resonant responses greatly. Figure 5.19-5.20 then show the damping and mass, given by equations (5.36) and (5.37), respectively, added to the first four modes of the beam when it is attached to the 0.005m thick plate. (In Figure 5.20, the dimensionless mass is defined to be the mass added divided by the mass density of the uncoupled beam). It can be seen that the added damping increases as the frequency increases while the added mass decreases as frequency. Therefore for high-frequency vibrations, the effect of coupling the plate to the beam is mainly to add damping to each vibration mode, whereas for low-frequency vibrations, the coupling effect can be considered as mainly adding mass to each mode. Both the damping and the mass added to the beam (by the coupling) are largest for its low order modes.

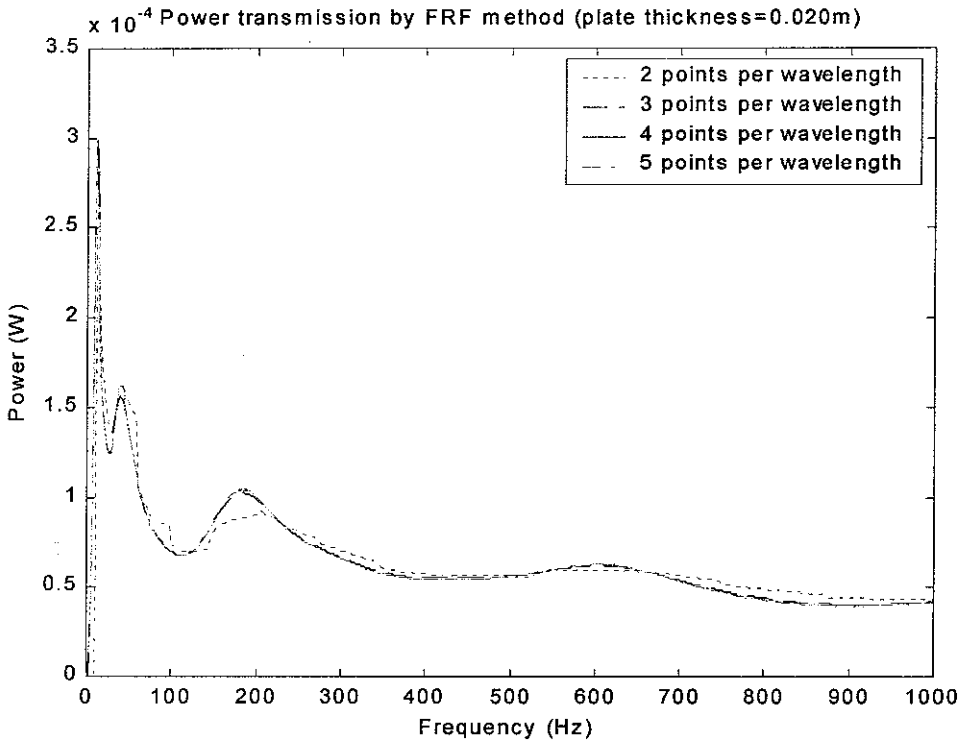

Figure 5.3

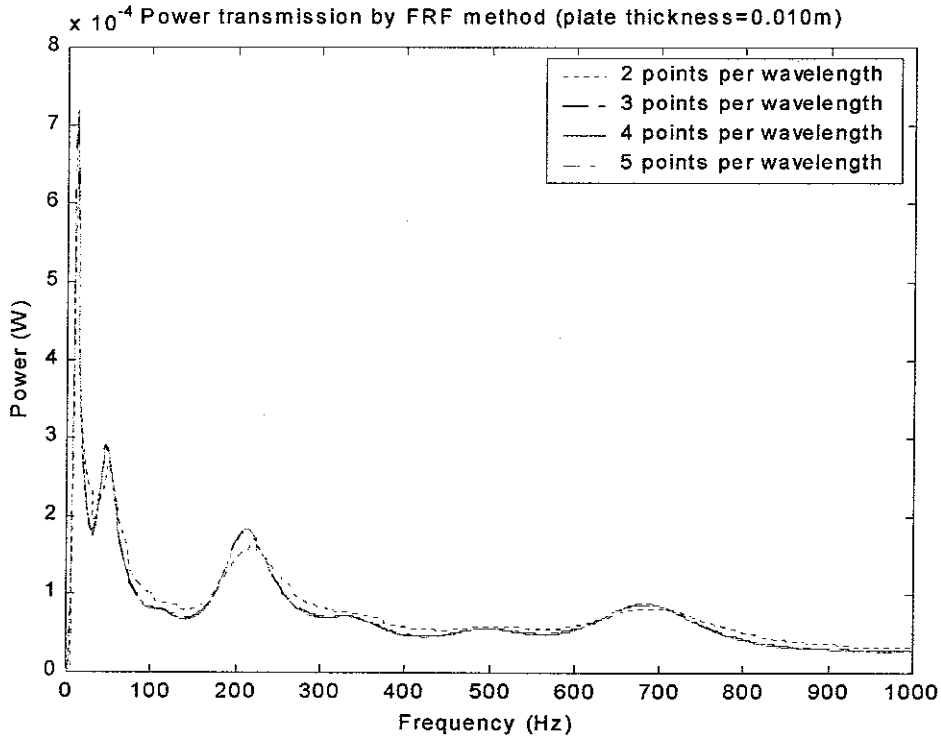

Figure 5.4

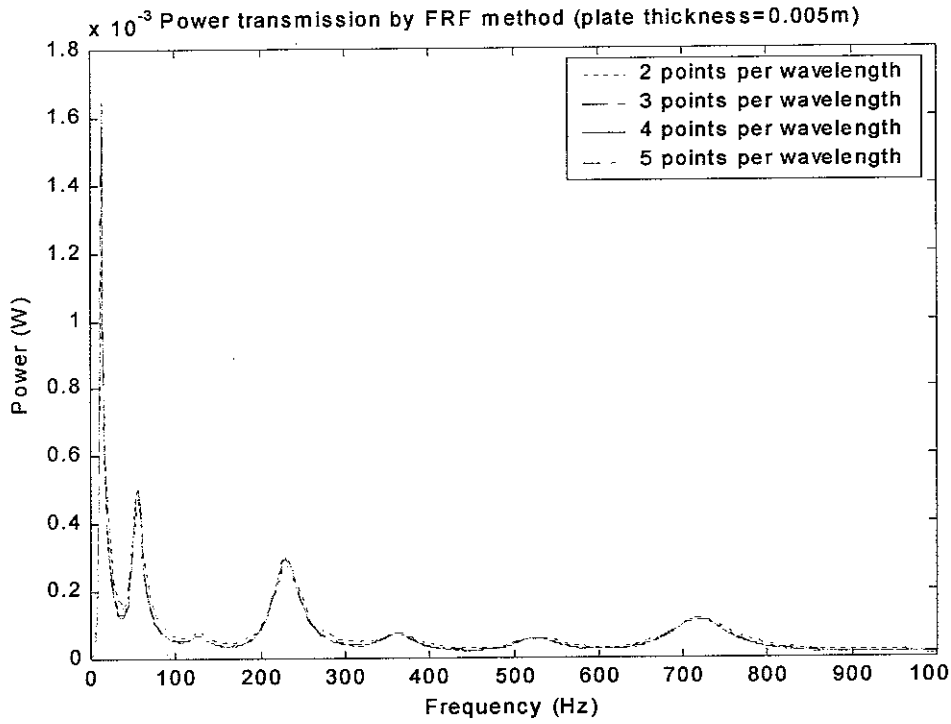

Figure 5.5

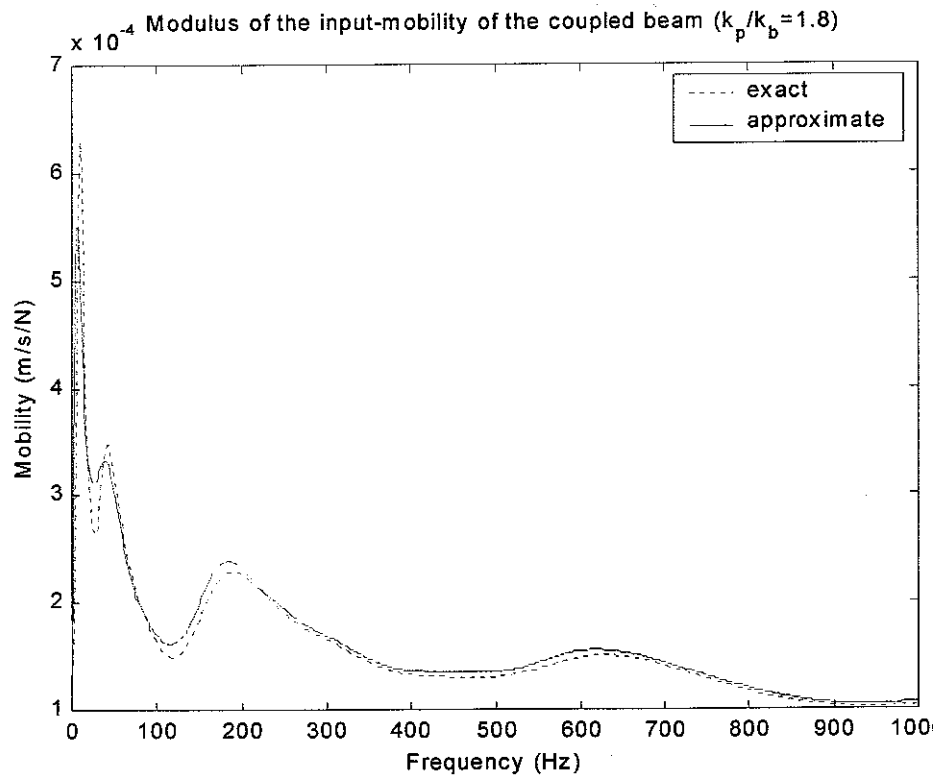

Figure 5.6

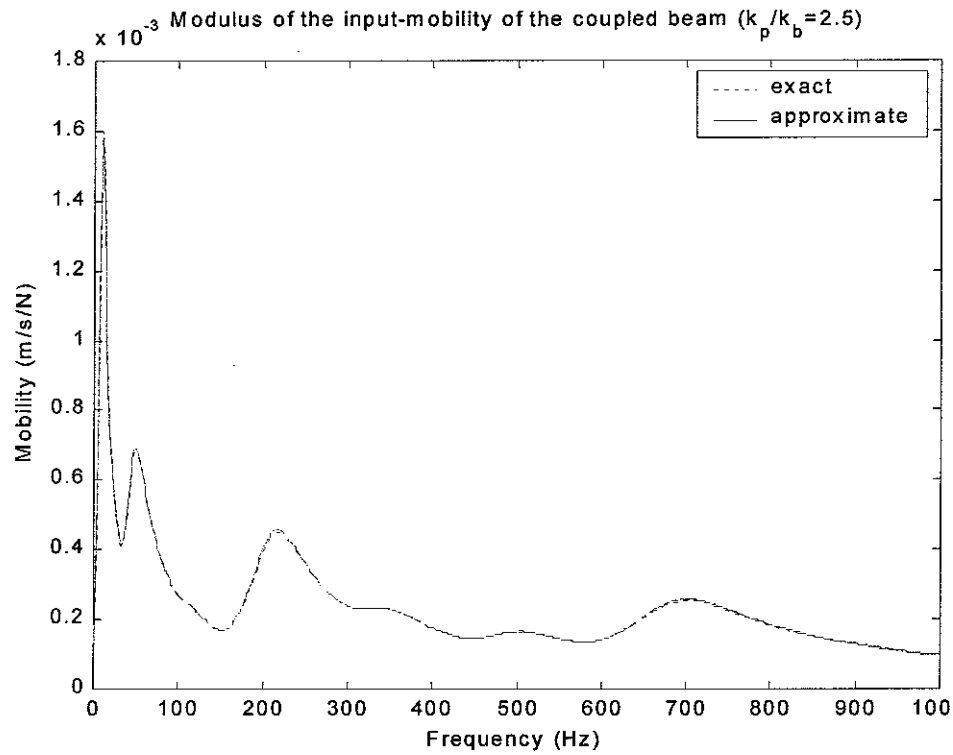

Figure 5.7

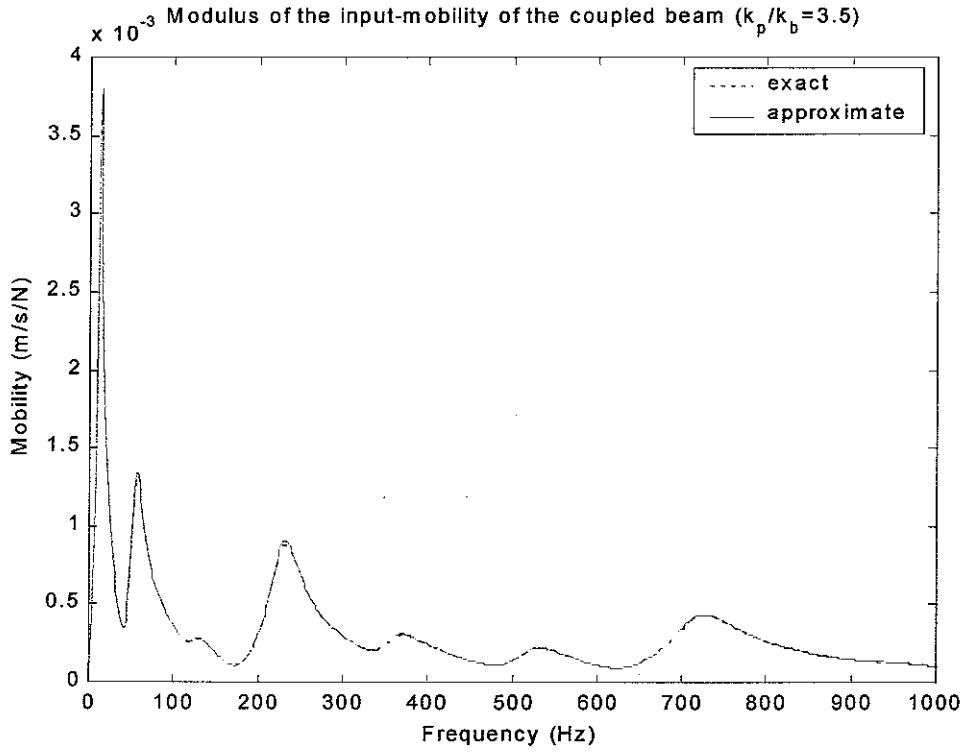

Figure 5.8

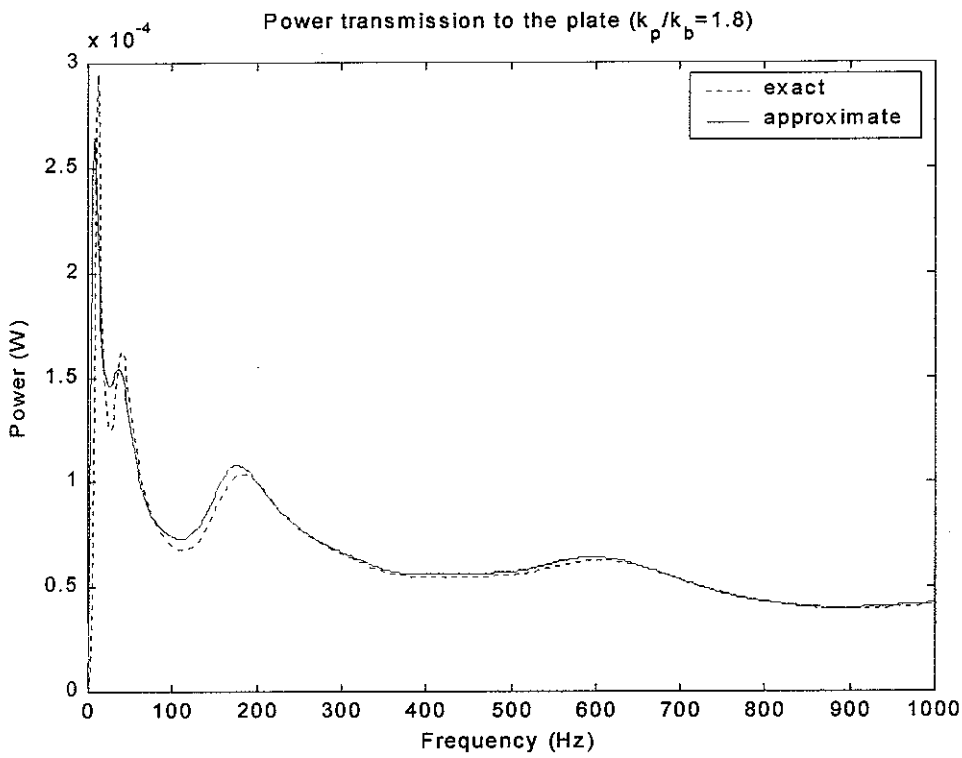

Figure 5.9

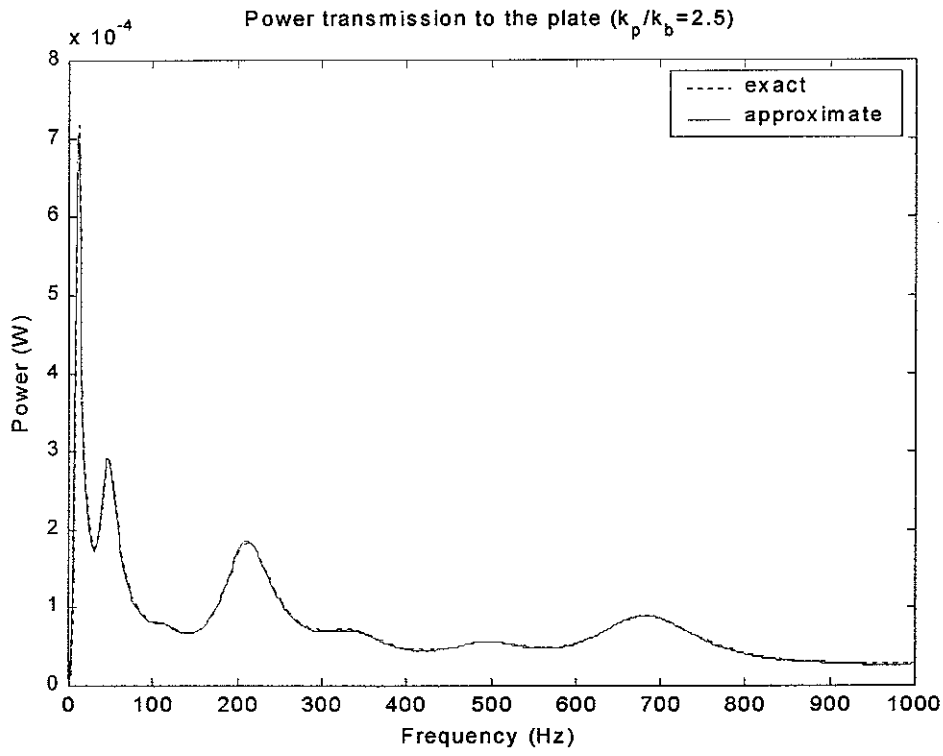

Figure 5.10

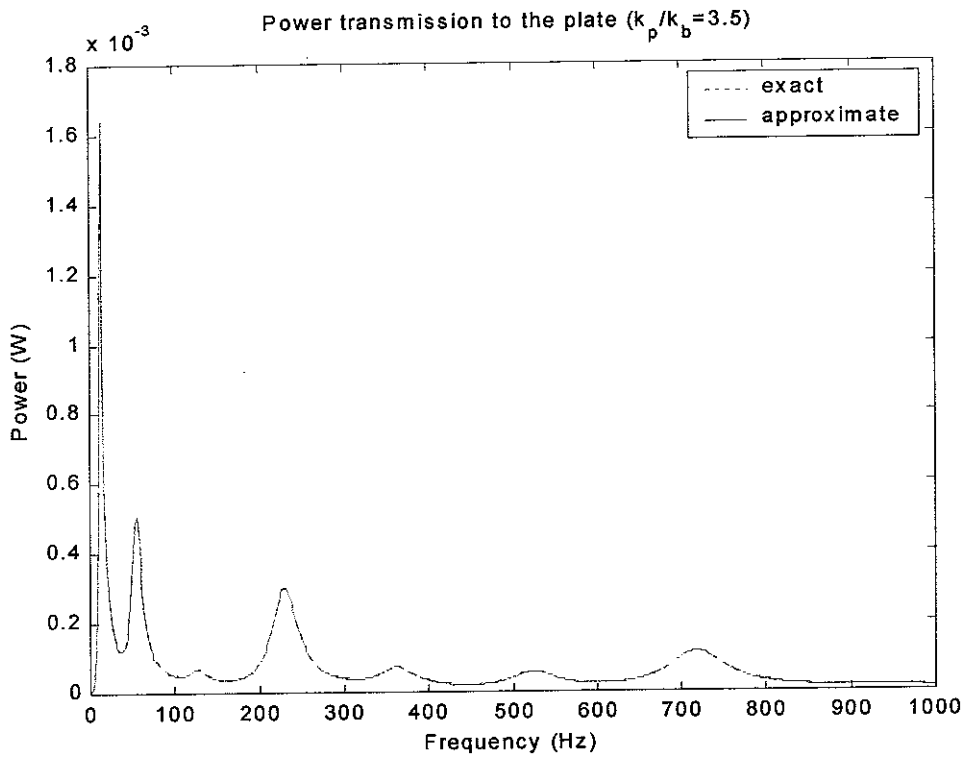

Figure 5.11

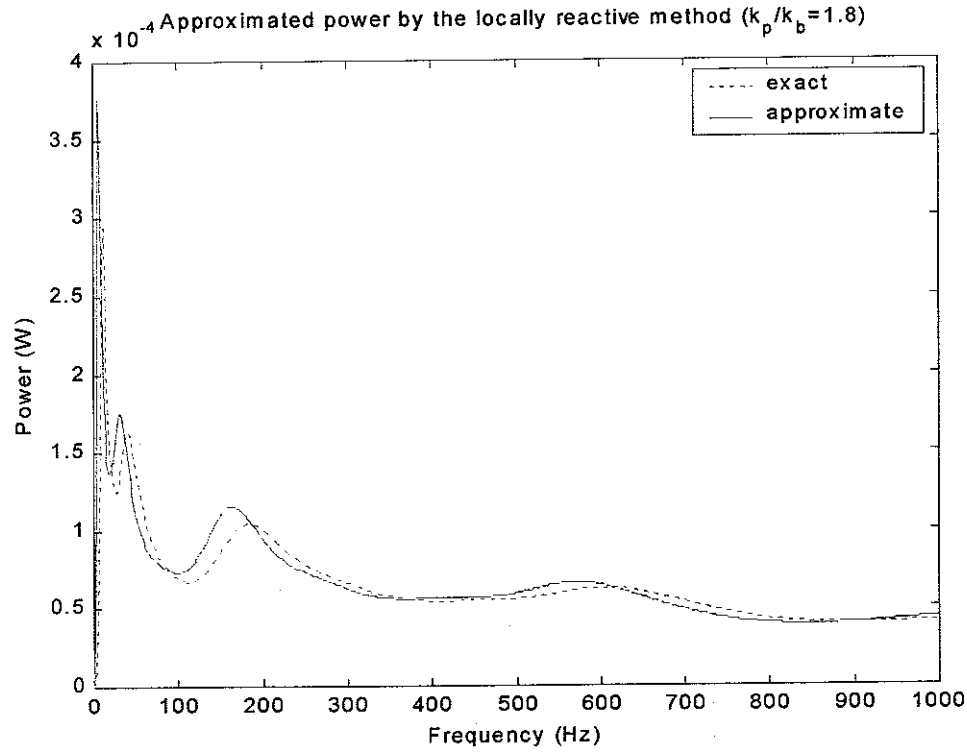

Figure 5.12

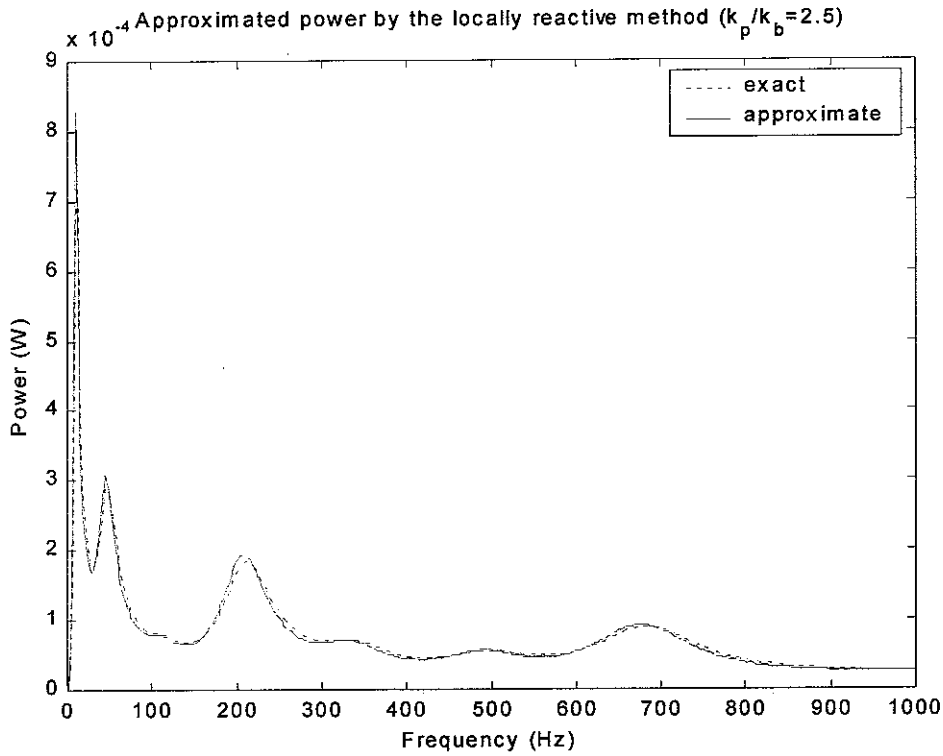

Figure 5.13

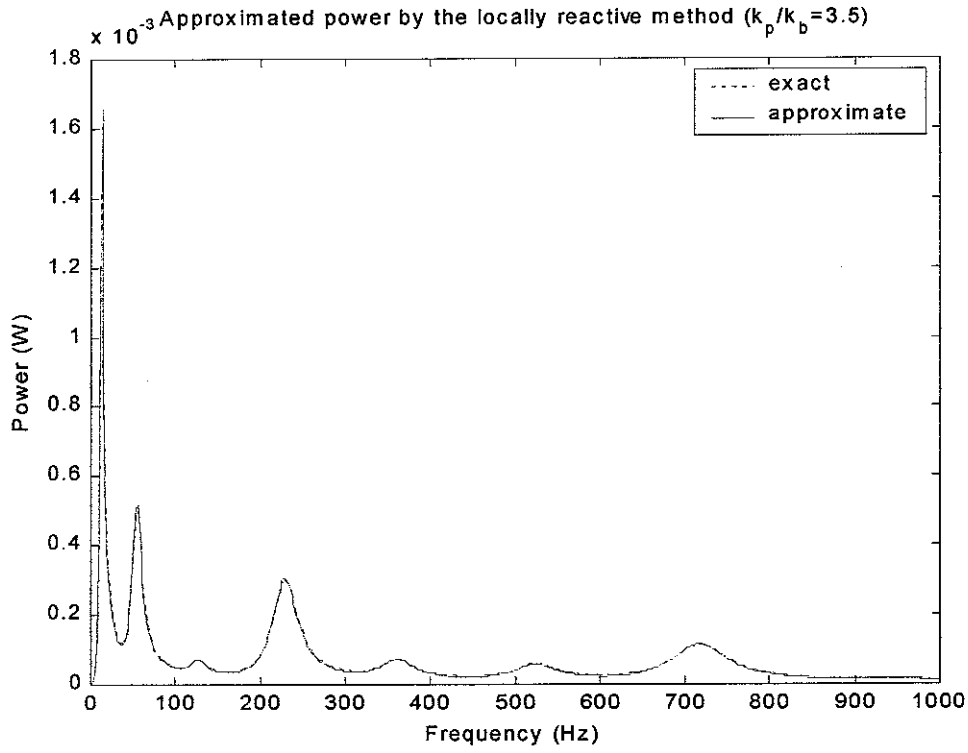

Figure 5.14

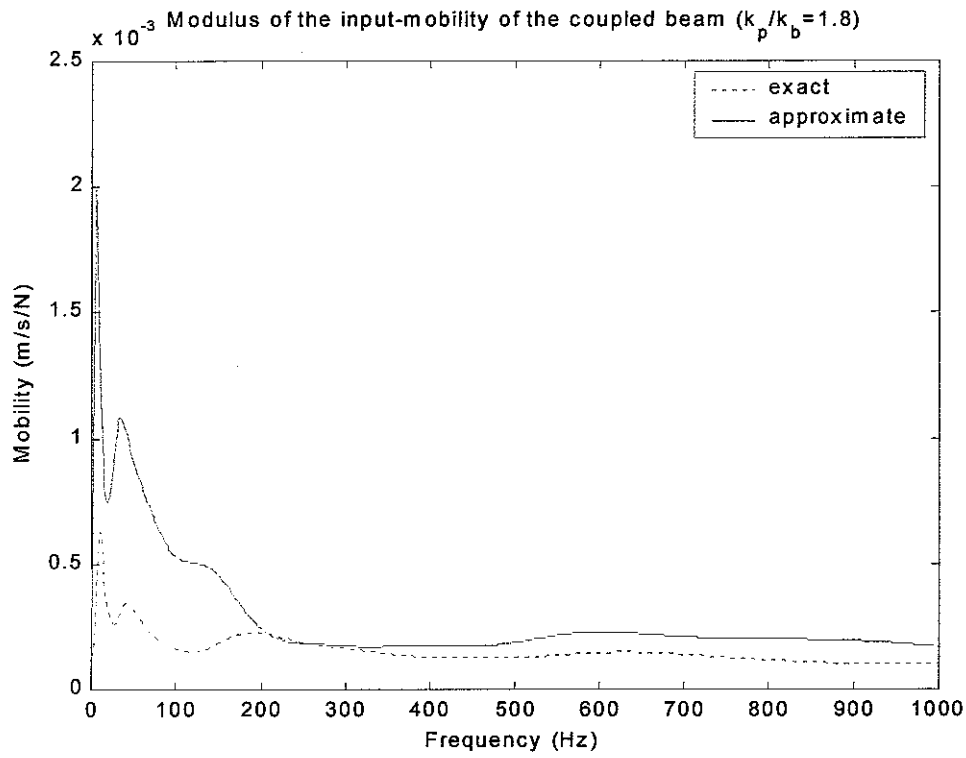

Figure 5.15

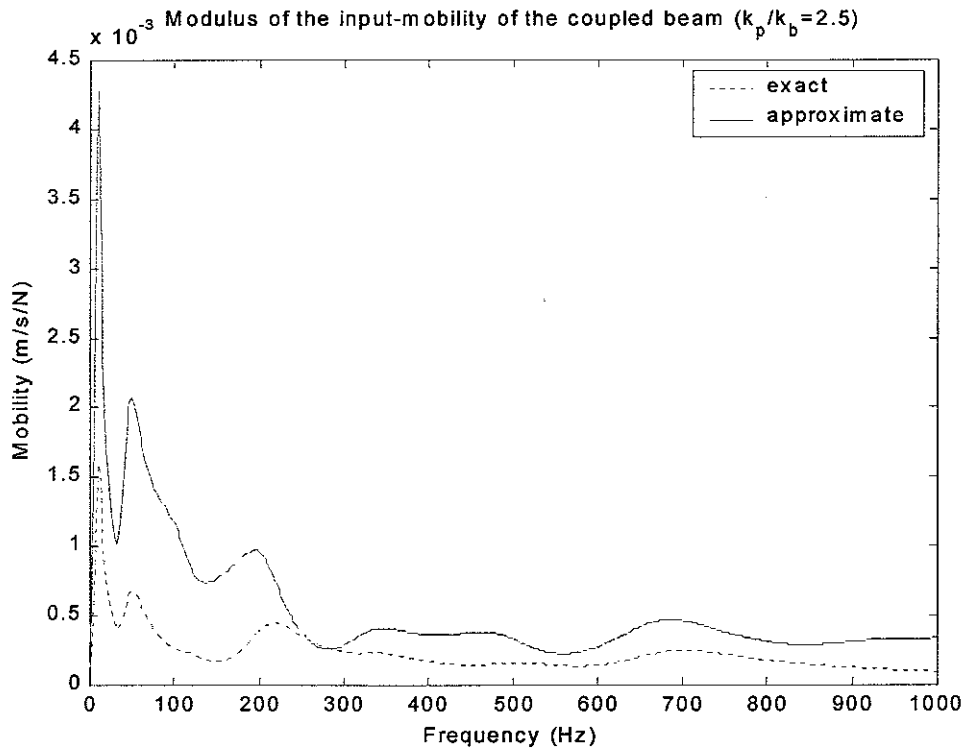

Figure 5.16

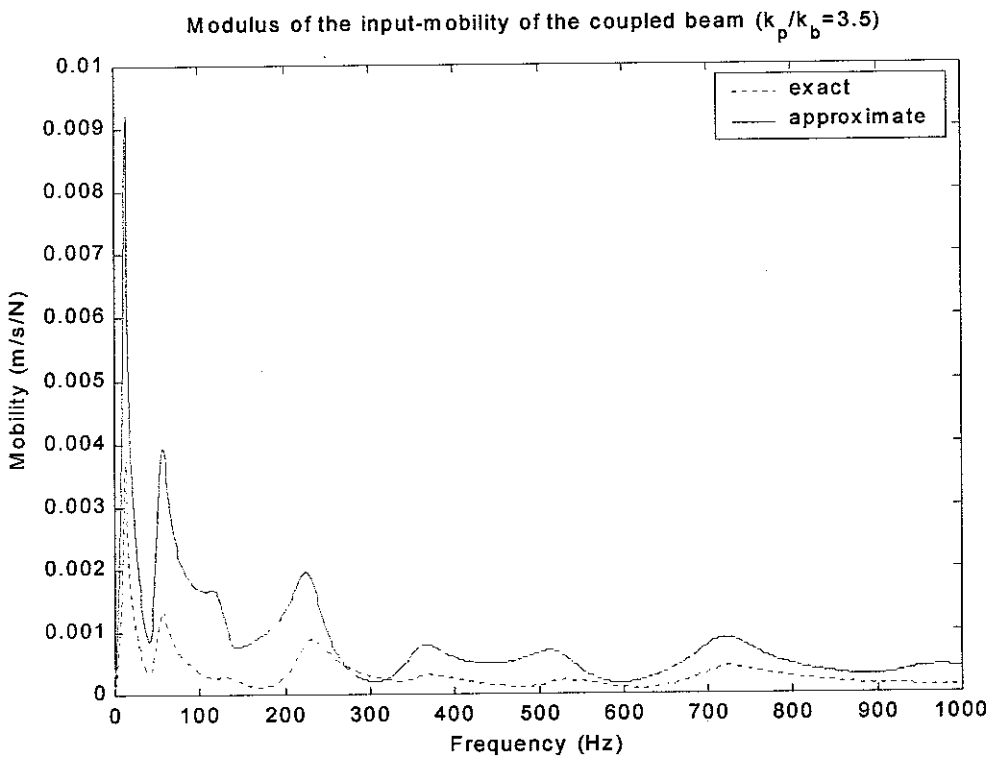

Figure 5.17

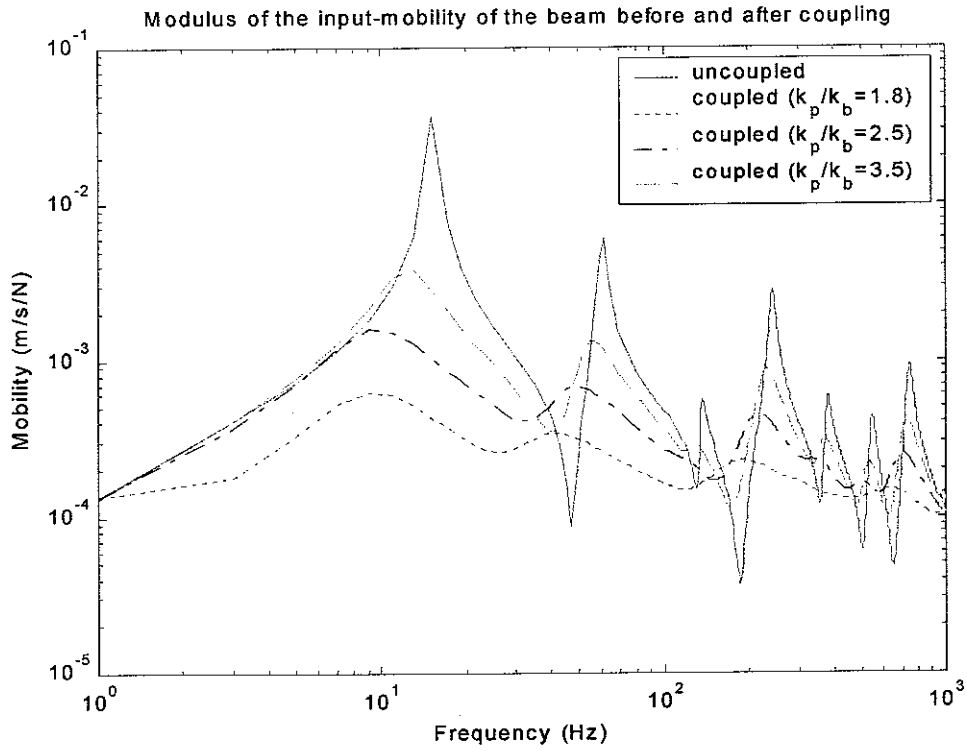

Figure 5.18

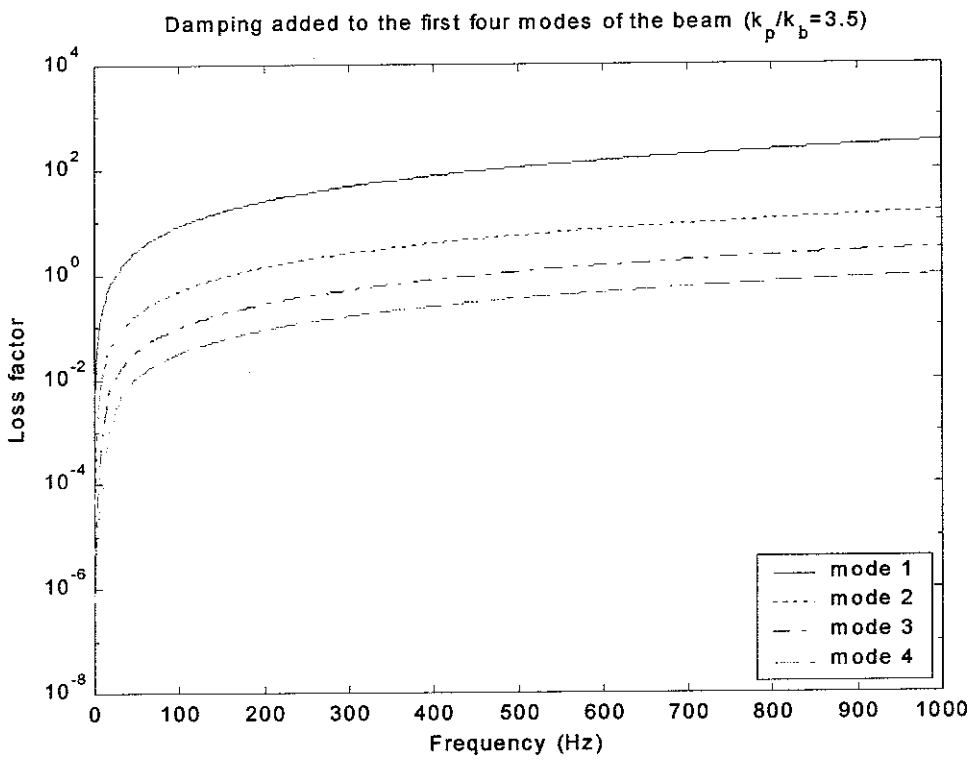

Figure 5.19

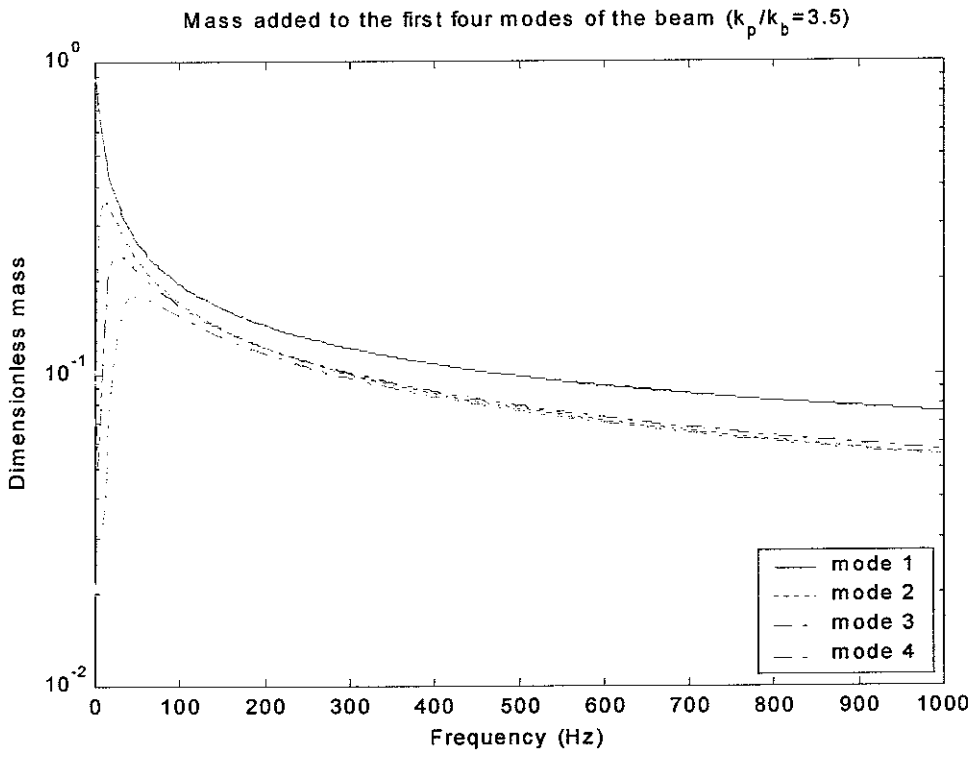

Figure 5.20

6. Power transmission through line couplings, Case 3: A finite beam attached to a finite plate

6.1 The modal analysis method

In Section 5 a combined modal analysis/Fourier Transform approach is developed to approximate both the dynamic response of the source beam and the power transmitted to the plate receiver. It is based on the assumption that the displacement of the receiver outside the coupling region can be ignored and the interface force and the interface displacement are then decomposed into a set of components in terms of beam modes. This technique has been shown to be quite accurate and efficient for various numerical examples. Therefore it is reasonable to suppose that similar approaches can be used to deal with such coupled systems as a finite beam attached to a finite plate by decomposing the interface displacement/force into a complete set of orthogonal functions. The modal analysis method of course will be one obvious choice to meet such a purpose, but this raises the question of whether the decomposition should be performed in terms of the beam mode shapes or the plate mode shapes. At the first stage of this study, a rectangular plate stiffened beam system is considered where the boundary conditions of the beam and of the plate (normal to the coupling) are the same. The plate modes are written using separation of variables, and the variation along the line of coupling is thus the same as that of the beam. It will be seen below that in this case, the analytical expressions for the dynamic response of the source beam and the transmitted power to the receiver can be derived very simply using the modal analysis method. The application of this technique to more general cases where a finite beam is attached a finite plate arbitrarily, is underway.

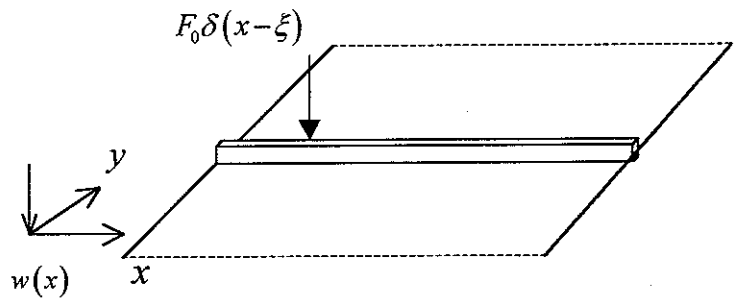

Figure 6.1 Line-coupled beam-plate system

For a coupled beam/plate system, as shown in Figure 6.1, the interface force is $f(x)$ (as shown in Figure 5.1), and the m th normalized mode shape of the beam is $\phi_m(x)$ so that

$$\int_0^{L_b} \phi_n(x)\phi_m(x)dx = \begin{cases} 1, & n=m \\ 0, & n\neq m \end{cases} \tag{6.1}$$

The vibration of the beam can then be written using equations (5.4)-(5.7) as

$$w_b(x) = \sum_n w_n \phi_n(x) \tag{6.2}$$

$$f(x) = \sum_n f_n \phi_n(x) \tag{6.3}$$

$$w_n = F_0 b_n \phi_n(\xi) - b_n f_n \tag{6.4}$$

where

$$b_n = \frac{1}{m_b} \frac{1}{\omega_n^2(1+j\eta_n)-\omega^2} \tag{6.5}$$

Let now assume $\Theta_k(x,y)$ be the k th normalized mode shape of the plate, and that it can be separated into the form

$$\Theta_k(x,y) = \varphi_m(x)\psi_r(y) \tag{6.6}$$

If

$$\varphi_m(x) = \phi_m(x) \tag{6.7}$$

i.e., the mode shapes of the beam and of the plate along the coupling are the same, then in this case each plate mode interacts with one and only one beam mode.

If y_0 is the coupling position in the plate, the force distribution on the plate is thus $f(x)\delta(y-y_0)$. By the modal analysis theory, the k th modal force on the plate is therefore

$$f_k = \int_{L_x}\int_{L_y} f(x)\delta(y-y_0)\Theta_k(x,y)dxdy \sum_k q_k \Theta_k(x,y) \tag{6.8}$$

Hence the plate displacement along the coupling region $y = y_0$, as shown in Figure 5.2, can then be written as

$$w_p(x,y_0) = \sum_k q_k \Theta_k(x,y) \int_{L_x}\int_{L_y} f(x)\delta(y-y_0)\Theta_k(x,y)dxdy \tag{6.9}$$

where $L_x = L_b$ and L_y correspond to the lengths of the plate along and normal to the coupling direction, respectively, and

$$q_k = \frac{1}{m_p} \frac{1}{\omega_k^{(p)^2}\left(1+j\eta_k^{(p)}\right)-\omega^2} \tag{6.10}$$

In the above equation, m_p, $\omega_k^{(p)}$ and $\eta_k^{(p)}$ are the mass density, the k th natural frequency and the corresponding loss factor of the plate, respectively. Combining equations (6.3) and (6.6)-(6.9), gives

$$w_p(x, y_0) = \int_0^{L_b} \left(\sum_n f_n \phi_n(x_0) \right) \left(\sum_m p_m \phi_m(x) \phi_m(x_0) \right) dx_0 \tag{6.11}$$

where

$$p_m = \frac{1}{m_p} \sum_r \frac{\psi_r^2(y_0)}{\omega_{m,r}^{(p)^2}\left(1+j\eta_m^p\right)-\omega^2} \tag{6.12}$$

and where $\psi_r(y_0)$ is the r th mode shape of the plate in y-direction normalized so that

$$\int_0^{L_y} \psi_n(y)\psi_m(y)dy = \begin{cases} 1, & n = m \\ 0, & n \neq m \end{cases} \tag{6.13}$$

Continuity of the displacement at the coupling gives

$$w_p(x, y_0) = w_b(x) \tag{6.14}$$

Combining equations (6.2), (6.11) and (6.14), then multiplying both sides of (6.11) by $\phi_n(x)$ and integrating along the length of the beam, leads to

$$w_n = f_n p_n \tag{6.15}$$

The above relation shows that the beam modes are still uncoupled after coupling with the plate, and p_n may be regarded as the line receptance of the plate to the n th mode of the beam which contains components from all those modes of the plate whose x-dependence is $\phi_n(x)$. Combining equations (6.4) and (6.15), the dynamic response of the coupled beam then can be written as

$$w_n = \frac{b_n}{1+b_n/p_n} F_0 \phi_n(\xi) \tag{6.16}$$

$$f_n = \frac{b_n}{p_n + b_n} F_0 \phi_n(\xi) \tag{6.17}$$

The power transmission from the beam to the plate can then be expressed as

$$P = \frac{1}{2}\mathrm{Re}\left\{\sum_n \int_0^{L_b} \left[f_n \phi_n(x)\right]^* j\omega \left[w_n \phi_n(x)\right] dx\right\} = \frac{1}{2}\mathrm{Re}\left\{j\omega \sum_n f_n^* w_n\right\} \tag{6.18}$$

Substituting equations (6.16) and (6.17) into (6.18), the power transmission can be written as

$$P = \frac{\omega}{2}\sum_n \left|\frac{b_n}{b_n + p_n} F_0 \phi_n(\xi)\right|^2 \mathrm{Im}\left\{p_n^*\right\} \tag{6.19}$$

From equation (6.12)

$$\mathrm{Im}\left\{p_n^*\right\} = \frac{1}{m_p}\sum_r \frac{\psi_r^2(y_0)\omega_{m,r}^2 \eta_p}{\left(\omega_{m,r}^2 - \omega^2\right)^2 + \left(\omega_{m,r}^2 \eta_p\right)^2} \tag{6.20}$$

Thus a simple analytical expression for the power transmission from a source beam to a plate receiver has been derived. Theoretically it is much more efficient and accurate than the FRF based sub-structuring method because it does not need to calculate the large mobility matrices of both the beam and the plate, and at the same time it avoids the process of matrix inversion which may provide inaccurate values caused by the ill-conditioned matrices.

6.2 The effect of coupling the plate to the beam

For the finite beam excited by a point force $F_0\delta(x-\xi)$, the displacements before coupling to the plate can be determined by

$$w_b(x) = \sum_n b_n F_0 \phi_n(\xi)\phi_n(x) \tag{6.21}$$

After coupling the displacement response is given by equation (6.16) as

$$w_b(x) = \sum_n b_n' F_0 \phi_n(\xi)\phi_n(x) \tag{6.22}$$

where

$$b_n' = \frac{b_n}{1 + b_n/p_n} \tag{6.23}$$

Let equation (6.5) be re-expressed as

$$b_n = \frac{1}{D_b k_n^4 (1 + j\eta_b) - m_b \omega^2} \tag{6.24}$$

where k_n corresponds to the wavenumber of the beam at its n th natural frequency. The term p_n of equation (6.12) can be expressed in the form

$$p_n = p_{n1} - p_{n2} - jp_{n3} \tag{6.25}$$

where

$$p_{n1} = \frac{1}{m_p} \sum_r \frac{\psi_r^2(y_0)\omega_{n,r}^2}{\left(\omega_{n,r}^2 - \omega^2\right)^2 + \left(\omega_{n,r}^2 \eta_p\right)^2} \tag{6.26}$$

$$p_{n2} = \frac{1}{m_p} \sum_r \frac{\psi_r^2(y_0)\omega^2}{\left(\omega_{n,r}^2 - \omega^2\right)^2 + \left(\omega_{n,r}^2 \eta_p\right)^2} \tag{6.27}$$

$$p_{n3} = \frac{1}{m_p} \sum_r \frac{\psi_r^2(y_0)\omega_{n,r}^2 \eta_p}{\left(\omega_{n,r}^2 - \omega^2\right)^2 + \left(\omega_{n,r}^2 \eta_p\right)^2} \tag{6.28}$$

Then b_n' can be written as

$$b_n' = \frac{1}{\left\{D_b\left[1 + j(\eta_b + \eta_n)\right] + D_n\right\} k_n^4 - (m_b + m_n)\omega^2} \tag{6.29}$$

where

$$\eta_n = \frac{1}{D_b k_n^4} \frac{p_{n3}}{(p_{n1} - p_{n2})^2 + p_{n3}^2} \tag{6.30}$$

$$D_n = \frac{1}{k_n^4} \frac{p_{n1}}{(p_{n1} - p_{n2})^2 + p_{n3}^2} \tag{6.31}$$

$$m_n = \frac{1}{\omega^2} \frac{p_{n2}}{(p_{n1} - p_{n2})^2 + p_{n3}^2} \tag{6.32}$$

Thus the coupling effects of the plate on the beam can be regarded as adding damping, stiffness, and mass to each mode of the beam, given by equations (6.30), (6.31) and (6.32), respectively. The energy dissipated by the added damping corresponds the energy transmitted from the beam to the plate.

6.3 Numerical examples

A numerical example comprising a finite beam attached to a rectangular plate as shown in Figure 6.2, is considered to investigate the efficiency and accuracy of this modal analysis based approach. For simplicity, both the ends of the beam and the four edges of the plate are chosen to be simply supported. The normalized mode shapes of the beam and of the plate is then

$$\phi_n(x) = \sqrt{\frac{2}{L_b}} \sin\frac{n\pi x}{L_b} \tag{6.33}$$

$$\Theta_k(x, y_0) = \varphi_n(x)\psi_m(y_0) = \left(\sqrt{\frac{2}{L_x}} \sin\frac{n\pi x}{L_x}\right)\left(\sqrt{\frac{2}{L_y}} \sin\frac{m\pi y_0}{L_y}\right) \tag{6.34}$$

Since $L_b = L_x$ here, the beam and the plate have the same spatial variation along the coupling, i.e., $\phi_n(x) = \varphi_n(x)$. In this case, the dynamic response of the coupled beam and the power transmitted to the plate can therefore be obtained using the analytical expressions described in Section 6.1.

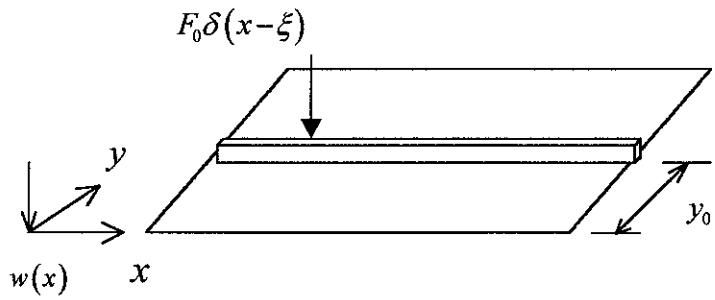

Figure 6.2 Line coupled simply supported beam/plate system

The numerical model chooses the same material (Perspex) and external force ($\xi = 0.73m$) as in the previous sections, and $y_0 = 0.45m$. All the other relevant parameters are listed in Table 6.1.

The dynamic response of the coupled beam and the power transmitted to the plate are firstly calculated using the FRF-based sub-structuring method where the line coupling is modelled by many discrete point couplings spaced at a quarter of the plate wavelength, and then predicted using equations (6.16) and (6.19) derived based on the modal analysis approach. Comparisons between the numerical solutions (FRF-based) and the analytical solutions (modal analysis based) are made in Figures 6.3-6.6. Figures 6.3-6.4 concern the

modulus of the input mobility of the coupled beam, and Figures 6.5-6.6 the transmitted power, corresponding to plate thickness 0.020m and 0.005m, respectively. It can be seen that the results by the two different approaches are almost exactly the same, but the analytical solution takes much less computing time than the numerical solution (e.g. only about one twentieth when the plate thickness is 0.005m). Theoretically the analytical solution is also more accurate than the FRF-based sub-structuring method because of the finite number of points used. Therefore this mode-based analytical approach is better than the FRF-based sub-structuring technique both in efficiency and in accuracy. However, it requires the beam and the plate mode shapes (along the coupling) to be the same.

Figure 6.7 are the input mobilities of the beam before and after coupling with the plate ($k_p/k_b = 1.8$ for the plate thickness 0.020m and $k_p/k_b = 3.5$ for thickness 0.005m), given by equations (6.21) and (6.22), respectively. It is similar to Figure 5.18 in that the effect of coupling the plate to the beam can be regarded as adding damping, mass and stiffness to the each mode of the beam. (In section 5, the added stiffness is considered to "block" the propagations of beam wave components with wavelengths shorter than the plate wavelength.) Figures 6.8-6.10 then show the damping, stiffness and mass, given by equations (6.30)-(6.32), respectively, added to the first four modes of the beam when it is coupled with the 0.005m thick plate. (In Figure 6.9, the dimensionless stiffness is defined to be the stiffness added divided by the stiffness of the uncoupled beam, and in Figure 6.10, the dimensionless mass the mass added divided by the mass density of the uncoupled beam.) It can be seen that both the damping and the stiffness are added to the low order modes of the beam, but the mass added tends to be independent of the mode order. This is in agreement with the case of a finite beam attached to an infinite plate. It also can be seen, surprisingly, that the maximum values for the added parameters occurs at 37, 120, 251, 429, 655 and 932 Hz but not at the natural frequencies of the uncoupled plate (these are listed in Table 6.2). Physically it means that the maximum coupling does not occur at the natural frequencies the uncoupled plate.

6.4 Summary and discussion

The dynamic analysis of a coupled beam/plate system can be greatly simplified by the modal analysis method if the mode shapes of the beam and of the plate (along the

coupling) are the same. In this case simple analytical expressions for the dynamic response of the coupled beam and the transmitted power to the plate can be found. Numerical examples have shown that this new mode-based approach is better than the classical FRF-based sub-structuring technique both in efficiency and in accuracy. Moreover, three analytical expressions for the damping, mass, and stiffness added to each mode of the beam are derived to simulate the coupling effects of the plate on the beam, as the other two cases investigated in the previous sections.

For a more general case of a finite beam attached to a finite plate, where the mode shapes of the beam and of the plate (along the coupling direction) are quite different, the equations of motion of the beam and of the plate tend to be coupled with each other, and the situation becomes more complicated. However, it might be still possible to simplify the vibration predictions by choosing appropriately a set of complete orthogonal functions along the coupling line, which will couple the 'unloaded' modes/waves of the beam/plate. This work will be done in the next stage of the research.

Table 6.1 Parameters of the numerical beam and plate structures

Structure	Beam	Plate
Dimension sizes	Length=2m; width=0.059m; Height=0.068m	Length=2m; Width=0.9m; Thickness=0.020m/0.005m

Table 6.2 Natural frequencies of the uncoupled plate (thickness=0.005m)

n \ m	1	2	3	4	5	6	7	8
1	7	25	54	96	149	214	291	380
2	11	28	58	99	153	218	294	383
3	17	34	64	105	159	224	300	389
4	25	43	72	114	167	232	309	398

Note: n denotes the mode order along x-direction, and m the order along y-direction.

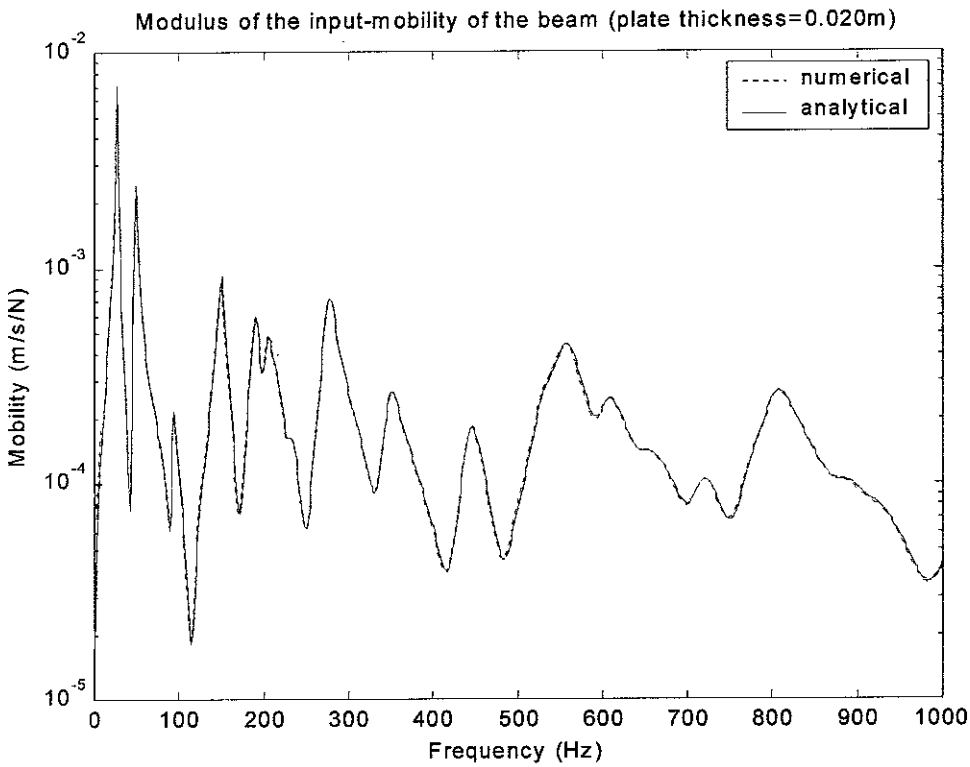

Figure 6.3

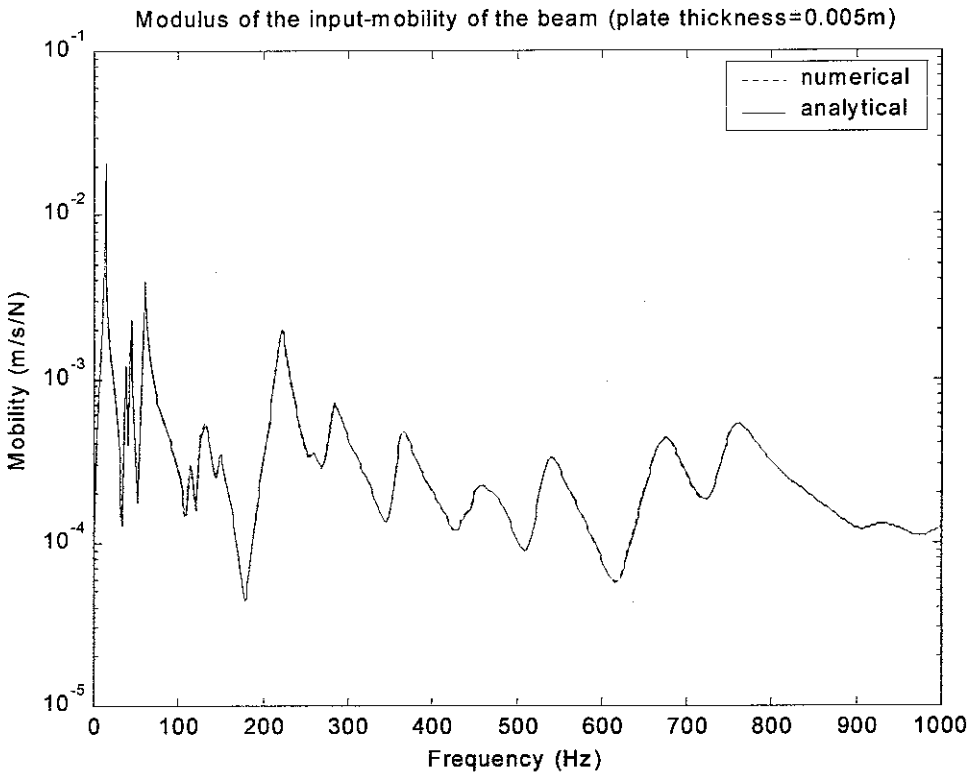

Figure 6.4

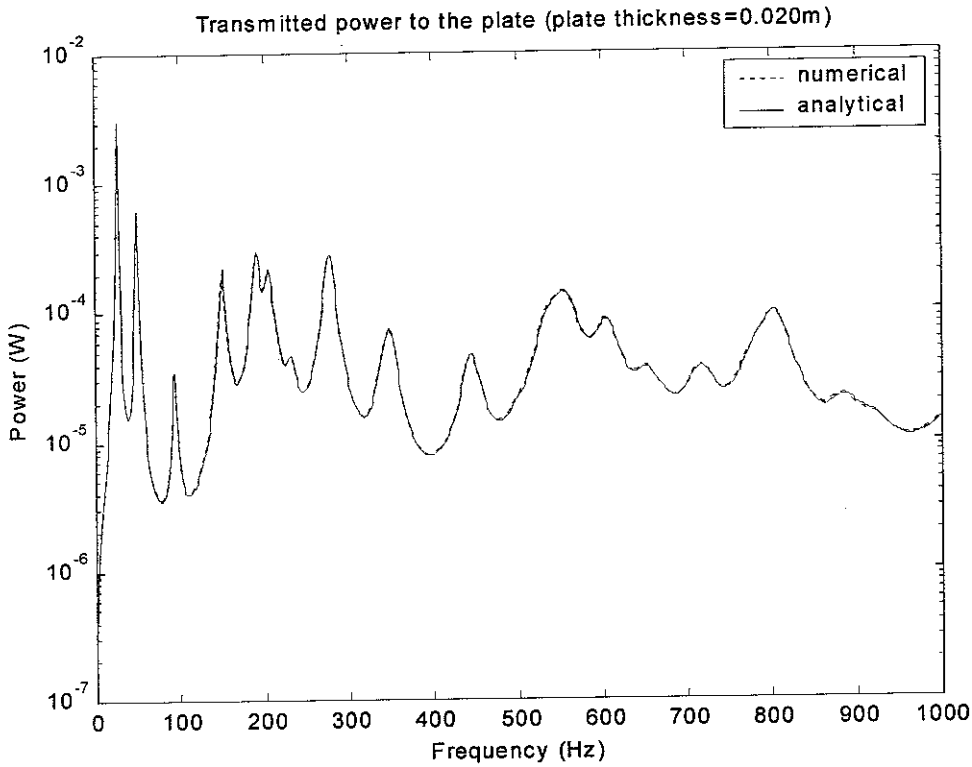

Figure 6.5

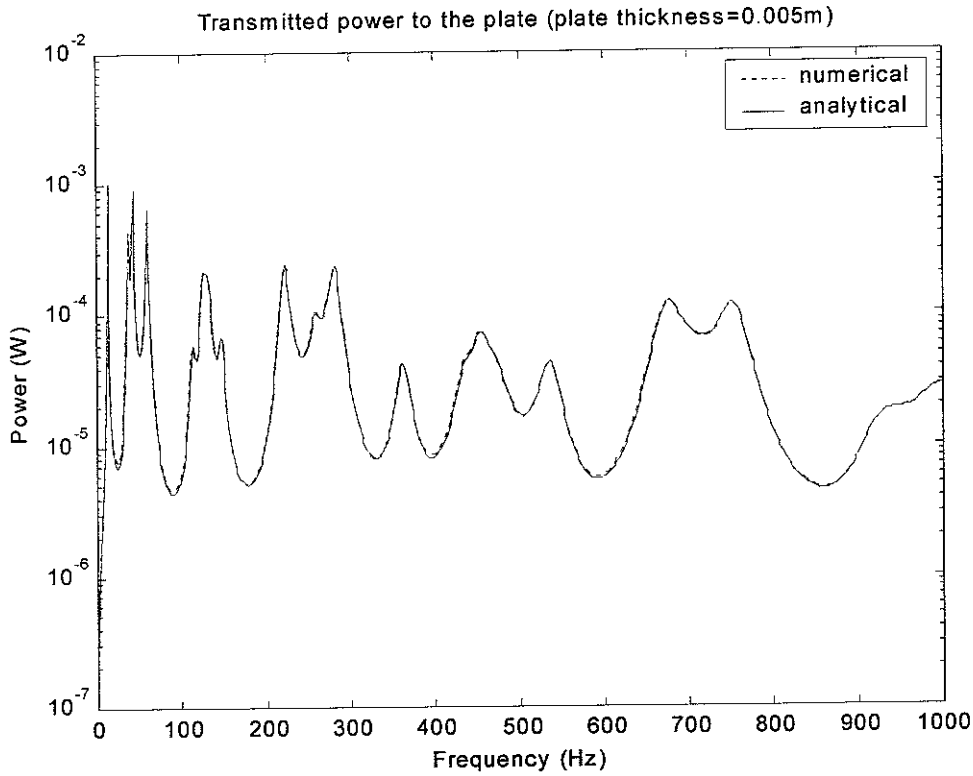

Figure 6.6

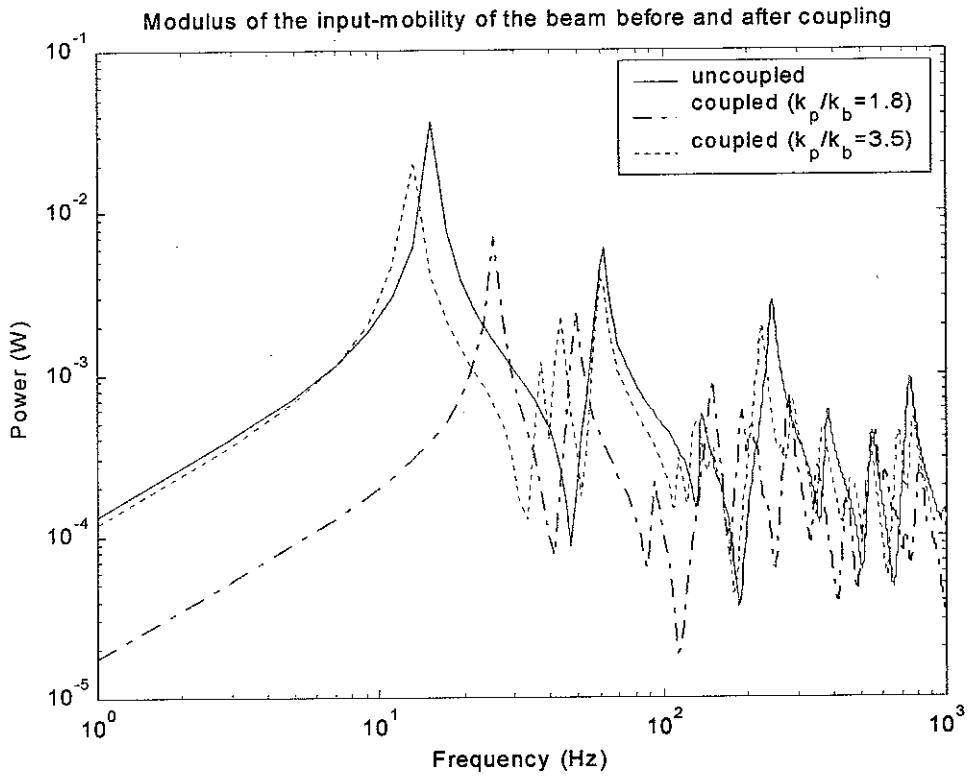

Figure 6.7

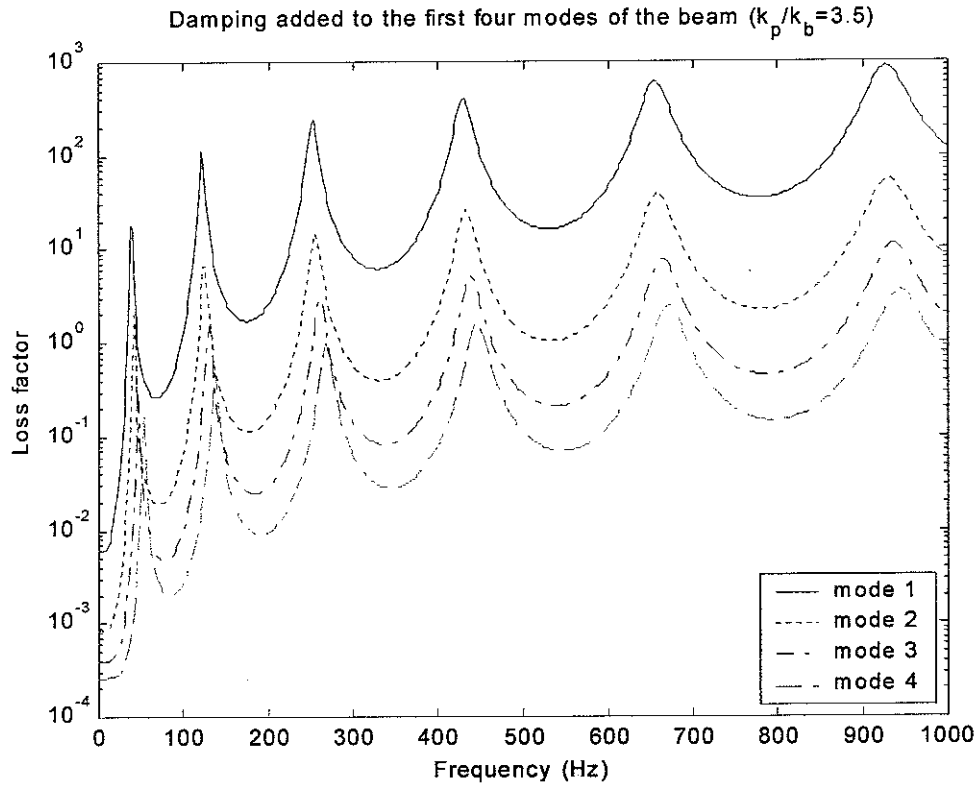

Figure 6.8

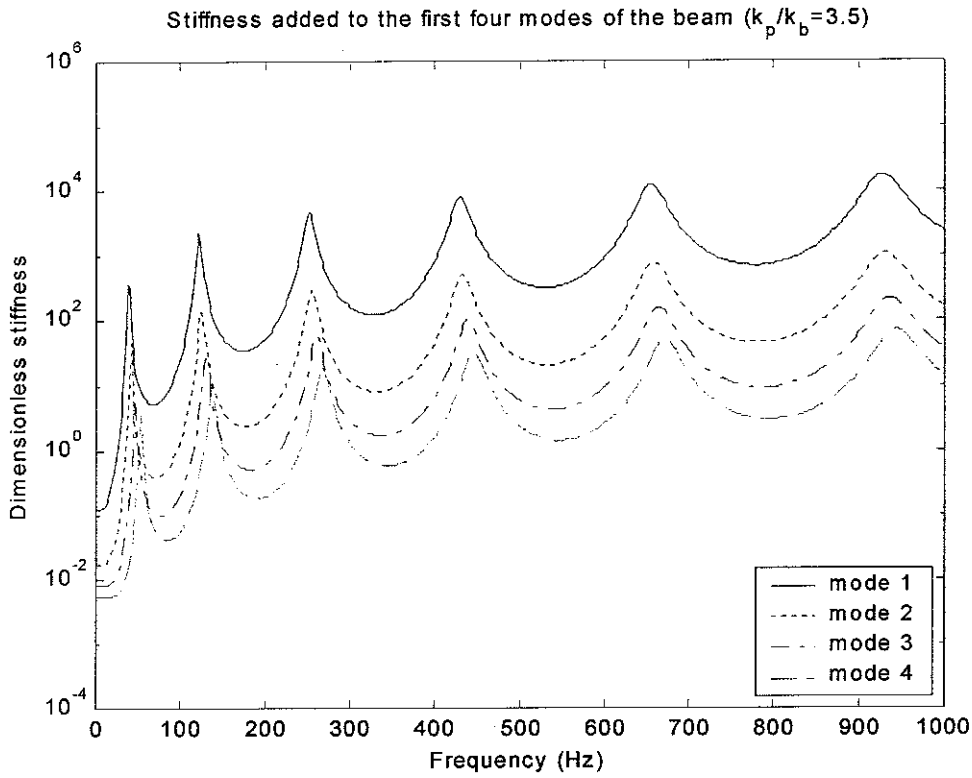

Figure 6.9

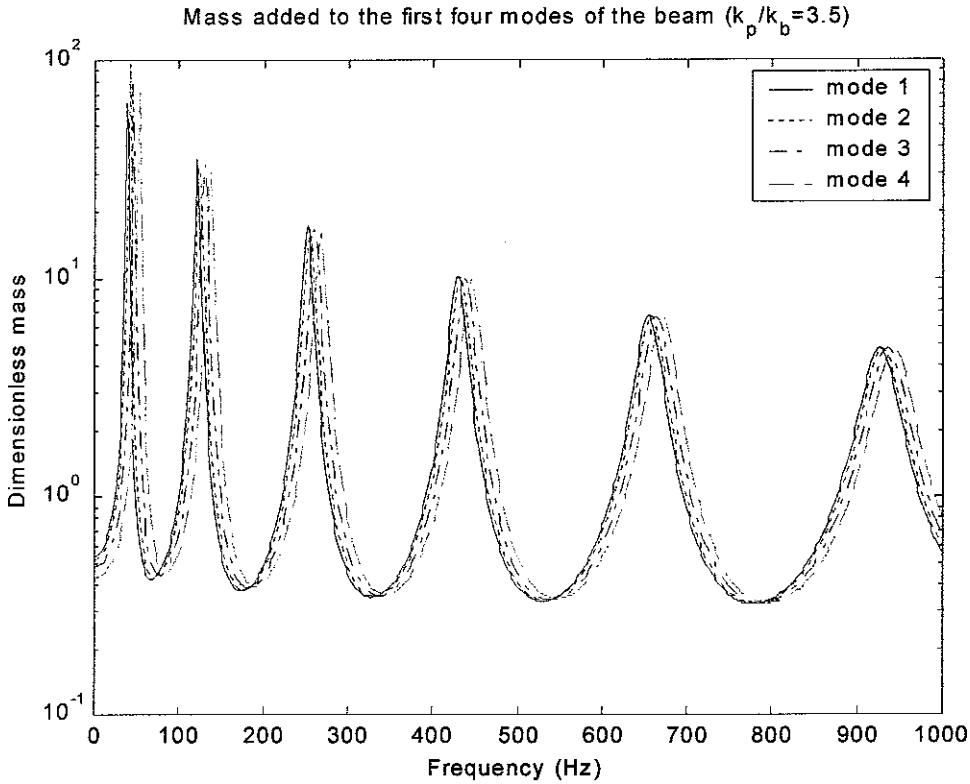

Figure 6.10

7. Conclusions

This study concerns approximating, simply and accurately, the power transmission of complex built-up structures consisting of long-wavelength source structures and short-wavelength receivers. For discrete coupling cases the multi-pole method and a new technique – the power mode method, have been investigated. For line-coupled cases, a foundation consisting of a beam-stiffened plate with the excitation applied to the beam was considered. The power transmission from the source beam to the plate receiver was investigated for three cases: Case 1, an infinite beam attached to an infinite plate, was investigated using the Fourier Transforms and wave analysis methods; Case 2, a finite beam attached to an infinite plate, was investigated by a combined modal analysis and Fourier Transform method; and Case 3, a finite beam attached to a finite plate, was investigated by a modal analysis method. Numerical examples were presented to verify the validity and accuracy of the various approaches, in which the classical FRF-based sub-structuring technique was used to provide a benchmark for the comparisons. For these the line couplings were modelled by discrete point couplings spaced a quarter of the plate wavelength apart. The main results are summarised below.

The transmitted power from a source structure to a receiver structure through discrete couplings can be approximated with acceptable accuracy using the multipole theory if either both the source and the receiver structures are fully symmetric, or the source structure is fully symmetric and the receiver has high modal overlap and does not show distinct resonant behaviour, or the source structure is much stiffer than the receiver which has high modal overlap and non-distinct resonant behaviour. For the remaining cases, the multipole method has no advantages over the FRF based sub-structuring method.

The power-mode method is another approach to predicting the power transmitted through discrete couplings. Three new approximation expressions for the power transmission have been derived: (1) The maximum and minimum power transmission can be simply approximated by upper and lower bounds. The practicality of these upper and lower power bounds depend on the width of this band. The stiffer the source and/or the more flexible the receiver, the narrower is this power band. (2) The frequency average power can be approximated quite accurately provided the receiver has high modal

overlap and is flexible enough compared to the source structure (e.g. the wavenumber of the receiver is three or four times that of the source structure). (3) When the receiver structure is much more flexible than the source so that it behaves in a 'fuzzy' manner, the power can be regarded as transmitted mainly by a set of free velocities, especially for the mid- and high frequency ranges.

For an infinite beam attached to an infinite plate, the Fourier Transform method is extremely useful. It has been found that only the wave components (of the beam) with wavelengths longer than the plate wavelengths can transmit power from the beam to the plate, and hence a good simplification can be made in the wavenumber domain to predict the power transmission. Similarly, the dynamic response of such a coupled beam/plate system can also be obtained by a wave-based approach in which the locally reacting theory can be derived when the plate wavenumber is much larger than the coupled beam wavenumber so that the line impedance of the plate is independent of the beam properties. Then the transmitted power to the flexible plate can be approximated simply. Moreover the effects of coupling the plate to the beam are discussed. Three expressions for damping, mass and stiffness have been derived to quantify how the plate loads the beam. It is found that the added damping depends on both the properties of the plate and the beam, whereas the added mass depends on the plate properties only.

For the case of a finite beam attached to an infinite plate, a combined modal analysis/Fourier Transform method has been developed to analyse the vibration relations between the subsystems by assuming that the displacement of the plate outside of the coupling region are ignorable. It has been found that very good approximations of the dynamic response of the coupled beam as well as the power transmission can be made with very low computational cost. The transmitted power can also be approximated based on the locally reacting impedance technique, i.e., the receiver is much more flexible than the source so that the correlations among the different points of the receiver (along the coupling) can be ignored. Since the mode/FT approach is to predict the vibration by decomposing the interface dynamic responses (both displacement and force) into the components of the beam modes so that the correlations among different components can always be ignored, due to the orthogonal property of modal shape functions, very good approximations can be made for both the modified dynamic response of the beam and the

transmitted power to the plate provided the only assumption holds, regardless the stiffness of the beam and/or the flexibility of the plate. Numerical study has shown that the assumption is not valid only for the very low frequency range where both the beam and the plate wavelengths are very long so that the plate displacements outside the coupling region are comparable with those of the coupling region. But for mid- and high frequency range, very good approximations can be made using the mode/FT approach, even when the receiver is not very flexible compared to the source structure. Of course the more flexible the receiver is, the more accurate the mode/FT approach is. The locally reacting approach, however, is not applicable for predicting the dynamic response of the source structure, even when the receiver is much more flexible than the source. Nevertheless, as far as the transmitted power is concerned, the locally reacting impedance method is a good approach to deal with such coupled system where the wavenumber of the receiver is at least twice that of the coupled source structure. The coupling effects of the plate on the beam can also be regarded as adding damping and mass to each mode of the beam. (The stiffness added is considered to block the short-wave-propagations of the beam.) The added damping depends on both the properties of the beam and of the plate (but almost regardless of the internal damping of the plate, which is in good agreement with the result obtained from fuzzy theory), and the added mass only depends on the properties of the plate as well as the mode shape functions of the source beam. As frequency increases, the added mass tends to depend on the plate properties only.

When both the beam and the plate are finite, the dynamic analysis of coupled system can be greatly simplified by the modal analysis method if the mode shapes of the beam and of the plate (along the coupling) are the same. In this case simple analytical expressions for the dynamic response of the coupled beam and the power transmitted to the plate can be defined. Numerical examples have shown that this new mode-based approach is better than the classical FRF-based sub-structuring technique both in efficiency and in accuracy. Moreover, three analytical expressions for the damping, mass and stiffness added to each mode of the beam are derived to simulate the coupling effects of the plate on the beam.

For a more general case of a finite beam attached to a finite plate, where the mode shapes of the beam and of the plate (along the coupling direction) are quite different, the

equations of motion of the beam and of the plate tends to be coupled with each other, and the situation becomes more complicated. However, it might still be possible to simplify the vibration predictions by choosing appropriately a set of complete orthogonal functions along the coupling line, which will couple the 'unloaded' modes/waves of the beam/plate. Further research, which forms the next stage of the study, is underway.

References:

1. E. E. UNGAR and C. W. DIETRICH 1966 *Journal of Sound and Vibration* 4, 224-241. High-frequency vibration isolation.

2. M. LALANNE, P. BERTHIER and J. D. HAGOPIAN 1984 *Mechanical vibrations for engineers.* Chichester, Wiley.

3. M. PETYT 1990 *Introduction to finite element vibration analysis.* Cambridge. MA: Cambridge University Press.

4. B. R. MACE *Structural Acoustics: Mechanical vibrations at higher frequencies*

5. F. J. FAHY 1994 *Phil. Trans. R. Soc. Lond* A 346, 431-447. Statistical energy analysis: a critical overview.

6. R. R. CRAIG JR. 1995 *Trans ASME Journal of Vibrations and Acoustics* 117, 207-213. Substructure methods in vibration.

7. R. R. CRAIG JR. 1987 *International Journal of Analytical and Experimental Modal Analysis* 2, 59-72. A review of time-domain and frequency-domain component-mode synthesis methods.

8. L. CREMER, HECKL and UNGAR 1988 *Structure-borne sound.* Berlin. Springer-Verlag. second edition.

9. R. J. PINNINGTON, R. A FULFORD and M. TERRY 1996 *Proceedings of inter-noise 96*, 1587-1592. The use of polar mobility for predicting the coupled response of machine mounting system.

10. B. R. MACE and P. J. SHORTER 2001 *Journal of Sound and Vibration* 242, 793-811. A local modal/perturbational method of estimating frequency response statistics of built-up structures with uncertain properties

11. R. M. GRICE and R. J. PINNINGTON 2000 *Journal of Sound and Vibration* 230, 825-849. A method for the vibration analysis of built-up structures, Part I: Introduction and analytical analysis of the plate-stiffened beam.

12. R. M. GRICE and R. J. PINNINGTON 2000 *Journal of Sound and Vibration* 230, 851-875. A method for the vibration analysis of built-up structures, Part II: Analysis of the plate stiffened beam using a combination of finite element analysis and analytical impedance.

13. A. D. PIERCE, V. W. SPARROW and D. A. RUSSELL 1995 *Trans ASME Journal of Vibration and Acoustics* 117, 339-348. Fundamental structural-acoustic idealisations for structures with fuzzy internals.

14. M. STRASBERG and D. FEIT 1996 *Journal of the Acoustical Society of America* 99, 335-344. Vibration damping of large structures induced by attached small resonant structures.

15. R. S. Langley and P. Bremner, 1999 *Journal of Acoustical Society of America* 105, 1657-1671. A hybrid method for the vibration analysis of complex structural-acoustic systems.

16. L. Ji, B. R. Mace and R. J. Pinnington 2001 *Technical Memorandum No.877, ISVR, Southampton University.* Vibration power transmission to flexible receivers from force sources.

17. H. R. Schwarz, H. Rutishauser, and E. Stiefel 1973 *Numerical analysis of symmetric matrices.* Prentice-Hall, INC. Englewood Cliffs, N. J.

18. J. H. Wilkinson 1965 *The algebraic eigenvalue problem.* Clarendon Press. Oxford.

19. E. Bodewig 1959 *Matrix Calculus.* North-Holland Publishing Company. Amsterdam.

20. A. T. Moorhouse and B. M. Gibbs 1993 *Journal of Sound and Vibration* 167, 223-237. Prediction of the structure-borne noise emission of machines: Development of a methodology,

21. X. Sheng, C. J. C. Jones and M. Petyt 1999 *Journal of Sound and Vibration* 228, 129-156. Ground vibration generated by a load moving along a railway track.

22. R. W. Ramirez 1985 *The FFT Fundamentals and Concepts.* Prentice-hall, Inc. Englewood cliffs. N.J.